NOAA Technical Memorandum ERL WPL-6

U.S. DEPARTMENT OF COMMERCE
NATIONAL OCEANIC AND ATMOSPHERIC ADMINISTRATION
Environmental Research Laboratories

Review of Electromagnetic Radiation Data From Severe Storms in Oklahoma During April 1970

WILLIAM L. TAYLOR

Wave Propagation
Laboratory
BOULDER,
COLORADO
June 1971

VIRONMENTAL RESEARCH LABORATORIES

WAVE PROPAGATION LABORATORY

NATIONAL OCEANIC AND ATMOSPHERIC ADMINISTRATION

BOULDER, COLORADO

U.S. DEPARTMENT OF COMMERCE
National Oceanic and Atmospheric Administration
Environmental Research Laboratories

NOAA Technical Memorandum ERL WPL-6

REVIEW OF ELECTROMAGNETIC RADIATION DATA FROM SEVERE STORMS IN OKLAHOMA DURING APRIL 1970

William L. Taylor

Wave Propagation Laboratory
Boulder, Colorado
June 1971

TABLE OF CONTENTS

REVIEW OF ELECTROMAGNETIC RADIATION DATA FROM SEVERE STORMS IN OKLAHOMA DURING APRIL 1970

William L. Taylor

The rate of occurrence of atmospherics in the 10 kHz to 10 MHz frequency range was examined for 6 severe storms and 8 non-severe thunderstorms during April 1970. Rates often exceeded 500/s in the VLF channels and 100,000/s in the HF channels for short time periods. The general characteristic of the rate data during non-severe conditions was that of a low background of atmospherics with occasional individual bursts of high rates produced by discrete discharges. Atmospheric activity greatly increased during severe conditions producing many more bursts per unit of time and resulting in an enhanced background of almost continuous high rate with little or no large individual bursts.

1. INTRODUCTION

The concentration of energy within the relatively small volume of a tornado has been the subject of much investigation by prominent scientists for more than a century, but this concentration has not been explained in terms of the energy budget. The power required to drive a tornado vortex has been estimated to exceed 10^8 kW (Vonnegut, 1960), yet this is small compared to the energy available in a single thunderstorm cell (Braham, 1952). Various theories have been proposed over the years suggesting that a tornado may be

driven by the kinetic energy resulting from the latent heat of condensation, the conservation of angular momentum, or the intense electrical activity associated with severe storms.

The electrical charges within a thunderstorm cloud are usually dispersed throughout the cloud or discharged to the earth by the discrete current surges of lightning strokes. Electromagnetic fields radiated during a lightning stroke, called atmospherics or simply sferics, contain frequency components extending from a few Hertz to many megahertz. Recent works related to the lightning discharge include, for example, that of Bradley (1965), Dennis and Pierce (1964), Iwata and Kanada (1967), Mackerras (1968), Muller-Hillebrand (1961), Ogawa and Brook (1964), Taylor (1963), and Uman and McLain (1969).

Jones (1959) reported that the occurrence rate of sferics in the 10 kHz region of the spectrum increased as the intensity of a thunderstorm increased, but decreased to a relatively small value prior to a tornado formation. However, the occurrence rate at 150 kHz greatly increased during the formation of a tornado. More recently, the effects observed on television sets tuned to channel 2 (54 MHz) have been reported by Waite and Weller (1969) and by Biggs and Waite (1970).

Many eyewitness accounts of unusual electrical activity in and around tornadoes have been reported during the last 20 or 30 years. Jones (1950) gives accounts of lightning and thunder being decidedly different during a tornado than during ordinary thunderstorms, for example, the presence of St. Elmo's fire in the vicinity of a tornado funnel, and the rapid rate of "one stroke right after another" at the base of a cloud just ahead of a funnel. Jones (1965) also reported nighttime observations of approximately circular patches of flashing pale blue illumination originating from within severe storms. Vonnegut (1960) presents a number of references which report tornado funnels

containing incessant lightning, a brilliant luminous cloud, and a ball of fire; and observations of St. Elmo's fire, a buzzing or hissing sound, odors of ozone or nitrogen oxides, and dehydration or burning of vegetation and soil along the path; all indicative of intense electrical discharges near and within the funnel.

Experimental evidence and eyewitness accounts of spectacular electrical displays accompanying tornadoes suggest that electrical energy in a tornado producing storm must be organized in a manner different from that usually accepted. If appreciable currents do flow either within or closely associated with the tornado funnel and dispersed into the severe storm cloud, the process might well tend to be almost continuous in the form of corona sparks or a gaseous glow. This would tend to reduce the energy radiated at lower frequencies from ground strokes and increase the energy partitioned into higher frequencies from short-distance, rapid-occurrence dispersive processes within the cloud.

To examine the possibility that distinguishable electrical radiation from severe storm areas could be found, indicating the spawning or existence of a tornado, a small effort was conducted during May 1969 in central Oklahoma. This initial work consisted of intermittent observations of the filter responses of 6 frequency channels in the 10 kHz to 500 kHz region using single stage filters with 1 kHz bandwidths. Although no tornadoes were confirmed within 100 km of the site during these observations, the sferics from numerous thunderstorms within 25 km were recorded. The analyses of these preliminary data as functions of amplitude and time revealed large variations in amplitude and high pulse repetition rates that often exceeded the capabilities of this original equipment. It was concluded

from the observations on regular thunderstorms that new equipment with greater dynamic range and with wider bandwidth filters extending to much higher frequencies would be required for examining the detail structures of the electromagnetic radiation from tornado supporting severe storms.

The purpose of this report is to give a non-detailed description of the equipment and recording techniques operated during the Spring 1970 tornado season in Oklahoma. The electromagnetic data obtained during periods of tornado activity and regular thunderstorm conditions within a range of 100 km during April 1970 are reviewed. The volume of data presented could certainly have been reduced and selectively presented to provide greater support for a hypothesis involving radio emissions from tornadoes. However, since the rate of occurrence data covering a wide band of frequencies and a large range of amplitudes are unique in the field of study at this time, it was desired to discuss only the data and the corresponding weather conditions in this report. A later report is planned to evaluate the use of electromagnetic radiation in identifying and tracking tornado activity.

2. INSTRUMENTATION

The design of equipment for the observation of electromagnetic radiation, or signals, from lightning discharges was dictated in part by results from the 1969 observations and by the need to record some parameter which may be more closely associated with thunderstorm activity than the amplitude response of a resonant circuit as a function of time. It was decided to observe the rate of occurrence and the

average number of responses of a resonant circuit per unit of time at 5 amplitude levels for each frequency channel extending from VLF into the VHF band.

A block diagram of the equipment is shown in figure 1 and a selection of circuit responses is shown in figure 2 to assist in presenting the basic atmospheric rate equipment. The transient signal arrives at the antenna, passes through the high input impedance antenna coupler, and is driven through several hundred feet of coaxial cable to the main equipment area. Inside the van, the gain is adjusted and the transient is distributed to several single stage tuned circuits which are resonant at the desired frequencies. The Q of each circuit is adjusted to the same value, this in turn will produce a bandwidth that is 10 percent of the center frequency. The signal is now presented to a logarithmic amplifier with a dynamic range exceeding 50 dB and is then rectified and smoothed. Five trigger circuits are individually adjusted to activate a one shot multivibrator each time the signal exceeds a predetermined level. The output of the one shot is integrated with a suitable time constant imposed and is presented to a data recorder through a logarithmic output driver.

The 25 μs time base for the circuit responses shown in figure 2 would be appropriate for a 1 MHz channel. A single transient is hardly recognizable in the rate data sample which is representative of a 0.01 second time constant. Overall measured response time to 90 percent of the final rate value of this equipment is about twice the time constant, which is 20 ms in this sample. Thus a burst of 200 sferics with an average separation time of 100 μs would produce a response equivalent to a rate of 9,000/s, i.e., 90 percent of 10,000. For very short duration bursts, therefore, the recorded rate may be less than the actual rate.

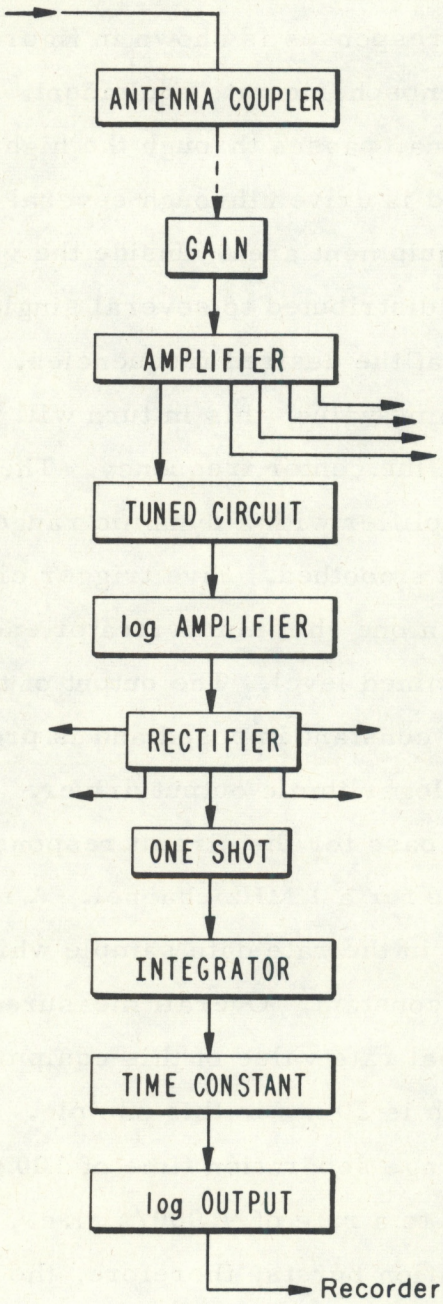

Figure 1. Atmospheric rate equipment simplified block.

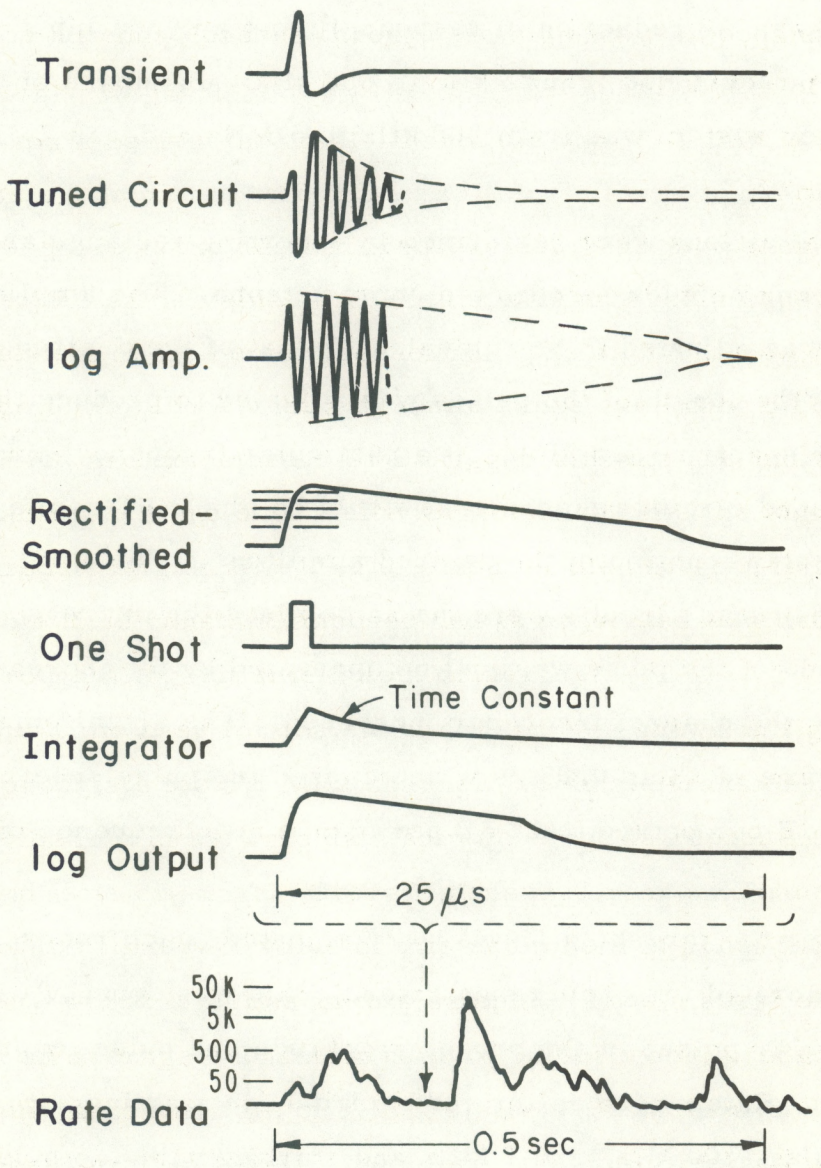

Figure 2. Atmospheric rate equipment circuit responses.

Two vertical monopole antennas with associated gain controls and amplifiers were used to cover the whole frequency band of interest. Each antenna was a 0.63 cm rod, one meter in length, with a 15 cm hemispherical corona cap at the top and an antenna coupler at the base. The antenna coupler was secured to a 4 ft square aluminum base and the whole unit enclosed in a plexiglass dome. The low frequency system bandpass (3 dB reduction in response) from antenna input to the amplifier output extended from 2 kHz to 600 kHz. Bandpass of the high frequency system was from 300 kHz to 5 MHz and was 7 dB down at 10 MHz.

Calibrations were performed by inserting rectangular pulses into the antenna coupler through a dummy antenna. The amplitude of the pulses was adjusted to be equivalent to that of the desired free space field. The length of the pulses was adjusted to produce the same Fourier spectrum amplitude at a particular frequency, and thus the same tuned circuit response, as would be obtained from a single voltage step function of the desired amplitude. The amplitude responses of all the tuned circuits were the same since the decrease in spectral amplitude of the pulse was just compensated by the increase in bandwidth as the channel frequency increased. The actual pulse used had a rise time of about 0.05 μs which caused the pulse spectrum to change from 6 dB per octave to 12 dB per octave at a frequency of about 5 MHz.

After the threshold levels were adjusted, each recorder response was calibrated for occurrence rates. This was done by using rectangular pulses of the proper amplitude and pulse length for each channel. Rates were calibrated each decade starting with 5 pulses/sec for 10 kHz, 100 kHz, and 1 MHz and starting with 1.6 pulses/sec for

all other frequencies. The maximum rate to which a set of channels could respond was limited by the bandwidth. As a guide, the maximum rate for which the channels were calibrated was limited to the bandwidth in Hertz divided by 2. The deflection representing the calibrated ratio for channels 11 and 12 with a zero level and a peak value of 5,000 is shown in figure 3. There are 3 marks between zero and 5 k (k = 1000), and these represent the other three decade rates of 500, 50, and 5 pulses per second. Similarly for channel 13, the peak value is 500 and the two other marks are for 50 and 5 pulses per second. For channel 14, there is only one mark between zero and the peak value of 500. This mark represents the next lower decade value below the value of the mark above it, which in this case will be 50 pulses per second. The 5 pulses per second mark is not shown because it is identical with zero. This channel and some of the others to be presented did not respond until the rate exceeded some value above 5 pulses per second. Channel 15 calibration rates are for zero and 50 with the decade value mark in between as 5 pulses per second. There was some noise on the channel 15 trace which was produced by instability in the output driver.

It is obvious from viewing the calibration rate marks in figure 3 that the deflections are not proportional to the logarithm of the rate. In general, the deflections are related linearly to the rate for the lower rates. As rate increases, a value is reached above which the deflection is logarithmically related to the rate. There is also a maximum deflection at which the recording apparatus limits. In general, the responses decay after a burst of atmospherics along a straight line; providing no further atmospherics exceed the threshold; until the low level linear region is reached and the decay becomes exponential.

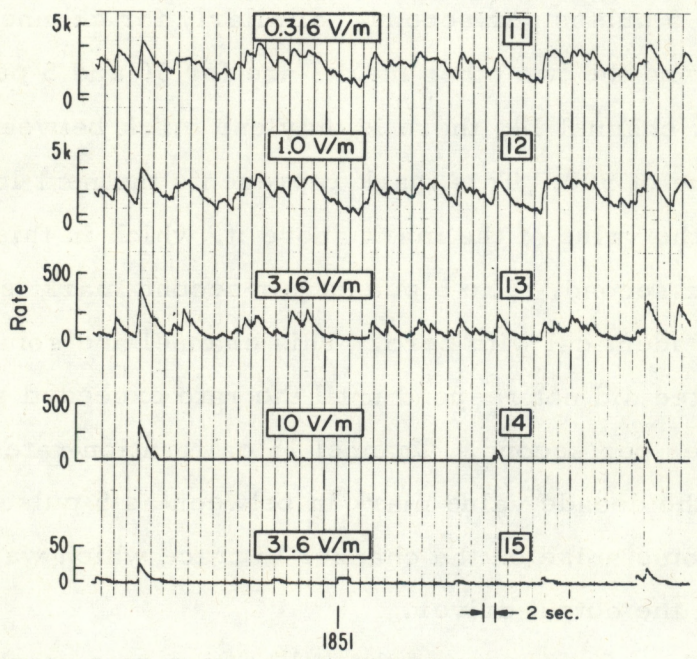

Figure 3. Sample Atmospherics Rate Data for 100 kHz, Slow Response on Expanded Time Scale from Fig. 4.

The time constants for each set of frequency channels were selected to smooth the data and yet allow the responses to vary fast enough to indicate some degree of detail in changing occurrence rates of the atmospherics. Electronic switching was used to change from a slow time constant, used primarily for low atmospheric rates during relatively inactive periods, to a fast time constant, employed when atmospherics were arriving at high rates during very active periods.

All of the rate data was recorded on FM magnetic tape at speeds of either 15/16 inch/s or 15/32 inch/s except for one channel of 3.16 MHz data and all of the 10 MHz data which was recorded on a paper chart recorder. The magnetic tape was played back at a speed of $7\frac{1}{2}$ inches/s for a non-detailed view of all recorded data. Of course, some of the peak rate values were not attained because of limitations in the frequency response of the paper chart recorder to the data played back at a speed-up factor of either 8:1 or 16:1. Certain limited time periods were selected for a more detailed view of the data, and these were transcribed onto paper charts by playing back tapes at 1 7/8 inches/s.

Time from a secondary time standard synchronized with NBS radio transmissions on WWV were mixed with one data channel on each tape recorder so that data could be correlated in time to an accuracy of a 1/10th second or so. These time codes took the form of a 2-second pulse each minute, a 4-second pulse each 10 minutes, and a 10-second pulse each hour.

The atmospheric rate data format used for presentation in this report is given in Table 1. The six FM tape recorders are designated by letters and the "16" represents the 16 channel paper chart recorder.

Table 1. Rate Data Format

Recorder	Channel No.	Frequency	Threshold v/m	Time Constants, seconds Slow	Fast
A	1	10 kHz	0.316	10.0	1.0
"	2	"	1.0	"	"
"	3	"	3.16	"	"
"	4	"	10.0	"	"
"	5*	"	31.6	"	"
B	6	31.6 kHz	0.316	3.0	0.3
"	7	"	1.0	"	"
"	8*	"	3.16	"	"
"	9	"	10.0	"	"
"	10†	"	31.6	"	"
C	11	100 kHz	0.316	1.0	0.1
"	12	"	1.0	"	"
"	13	"	3.16	"	"
"	14	"	10.0	"	"
"	15*	"	31.6	"	"
"	16	316 kHz	0.316	0.3	0.03
D	17	"	1.0	"	"
"	18	"	3.16	"	"
"	19	"	10.0	"	"
"	20*	"	31.6	"	"
"	21	1.0 MHz	0.316	0.1	0.01
"	22	"	1.0	"	"
E	23	"	3.16	"	"
"	24	"	10.0	"	"
"	25*	"	31.6	"	"
"	26	3.16 MHz	0.316	"	"
"	27	"	1.0	"	"
"	28	"	3.16	"	"
"	29	"	10.0	"	"
16	30	"	31.6	"	"
"	31	10.0 MHz	0.316	"	"
"	32	"	1.0	"	"
"	33	"	3.16	"	"
"	34	"	10.0	"	"
"	35	"	31.6	"	"

Data channels that also contain time are indicated by an asterisk (*). The cross (†) by channel 10 indicates that the time marks were removed from channel 8 and placed on channel 10 after the observations on April 18.

An example of atmospheric rate data for the five amplitude levels ranging from 0.316 v/m to 31.6 v/m for the 100 kHz channel is shown in figure 4. During this period of about 30 minutes when the atmospheric activity was not changing rapidly, the integrator time constant was changed at 1850 GMT from a fast 0.1 second value shown on the left to a slow 1.0 second value shown on the right. All data times are given in Greenwich mean time which is six hours later than Central Standard Time. Calibrated levels of occurrence rates are shown on the left for the fast time constant and on the right for the slow time constant. The vertical brackets shown near the times 1842 and 1851 indicate the selected portions of data to be presented in other figures for more detail using an expanded time scale.

The detail data for the 1851 time bracket of the 100 kHz sample are shown in figure 3 where the top two traces, marked as channels 11 and 12, are for the two lowest threshold levels and indicate by their similarity that few additional atmospherics were received at this time with amplitudes less than 1.0 v/m. These traces show that a few atmospherics at these levels were arriving within time periods short with respect to the recovery time imposed by the one second time constant. Channel 13 shows numerous periods when few, if any, atmospherics arrived that exceeded 3.16 v/m. Channels 14 and 15, as would be expected for higher threshold levels, show only occasional short bursts of activity.

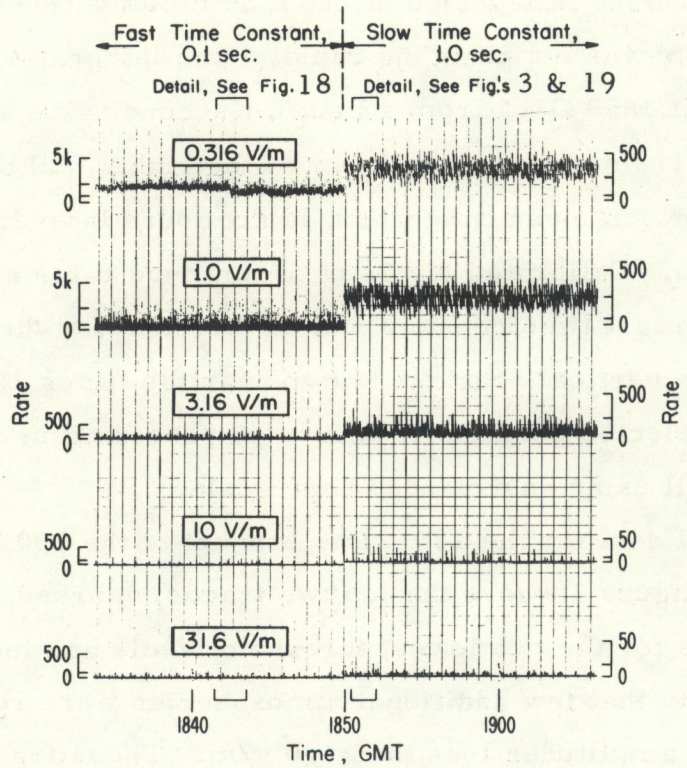

Figure 4. Sample Atmospherics Rate Data for 100 kHz, Comparing Fast and Slow Time Constant Responses

Various other parameters were recorded on the 16 channel paper chart recorder. The potential gradient or vertical electric field was recorded as channel 38. A deflection in the positive direction represents positive charge moving away from the site. The X (north) and Y (east) components of the earth's magnetic field were recorded as channels 39 and 40, respectively. A positive or upward deflection represents an increase in field.

Other measurements were made but will not be presented as data at this time for various reasons. Integrated noise channels at 10 kHz, 100 kHz, 1 MHz and 10 MHz were not sensitive to variations in atmospheric activity independent of distance to the storms and appeared very inferior to the rate data at the same frequencies. The rate data channels for 31.6 MHz proved to be unreliable. Instabilities in the rate circuits coupled with the necessity for increased gain to overcome the role-off characteristics of the system resulted in spurious noise being observed on all but the highest amplitude channel. Repeated difficulties with the antenna and the converter for the 137 MHz rate channels prevented observing more than just a few scattered minutes of reliable data.

Direction of arrival (DF) was observed using crossed loop antennas. Low frequency measurements were made wideband and at 10 kHz and 100 kHz using one set of loop equipment, and measurements at 1 MHz and 10 MHz were made using another set of equipment. The loop antennas were 0.7 meters square in an electrostatic shield with 16 turns for the LF loop and 2 turns for the HF loop. The data were recorded by photographing the DF presentations on several oscilloscopes using 35 mm cameras. The cameras were intermittently operated in an open shutter strip-film mode at a film transport

speed of 25 cm/s or operated at one time exposure frame each second. In either case, it is a monumental task to scale and interpret such data, and this has not been attempted to date. Time exposures of several minutes, however, were also obtained and some of this data will be presented.

Two black and white television receivers were operated from separate rotating directional antennas and the TV picture tube was photographed intermittently with a 35 mm camera. One TV set was always tuned to channel 2 and the other set tuned to either channel 5 or 7. No prolonged brightening of the TV tube was observed but only the occasional lightning flash bars were recorded. These data will not be presented at this time.

The atmospheric rate, potential gradient and magnetic field data presented in this report were reproduced from the paper chart records obtained by direct recording of the data or by transcription from magnetic tapes. These reproductions were cut into narrow strips and presented in a single figure for a particular observation to assist the eye in following the related details of the data as a function of time. Because of slight variations in chart speeds and photographic reproductions, the data do not always exactly line up in time. Channel 1, 0.316 v/m at 10 kHz, is presented at the top and channel 40, Y component of the magnetic field, presented at the bottom when available. A channel or group of channels was omitted whenever interference, or equipment malfunction produced unreliable data, or because there was no response to a particular parameter. Scales for the rates generally alternate from side to side, with the rates for the odd numbered channels given on the left side and the rates for the even numbered channels given on the right side. Brackets at the top and

bottom of the figures indicate where a slab of data was selected for detailed or expanded time presentations. Time and date at the bottom of each figure are given in Greenwich mean time, GMT. Channel 25 is always presented, even when no data are present, as an additional time channel.

3. OBSERVATIONS

The recording equipment was usually activated when there was a chance of thunderstorms within 200 km of Norman. Thunderstorm areas were tracked by associating the observations of atmospheric activity from the wideband DF display with precipitation returns from weather radar operated by NSSL. Equipment calibrations required about an hour, often more time when adjustments were necessary, and every effort was made to have all data channels operating properly before beginning the observations. Actual data recording was started when thunderstorm activity began to either grow within or move into the general Oklahoma area and the recording was ended when the activity began to dissipate or move outside the range of interest.

During the 1970 spring tornado season in Oklahoma, 93 hours of observations were recorded during 13 periods of activity in April and May. The data presented in this report will include only those obtained from 47 hours of observation during 7 periods in April.

3.1 The April 16-17 Severe Storm

Observations began at 1735 GMT with the first atmospheric activity of the season. Thunderstorms became more numerous in central Oklahoma as the day progressed, but no well organized line formed. Radar indicated the precipitation was generally moving toward the ENE at about 45 km/hr (25 knots) with showers occasionally near Norman. Local atmospheric activity began around 2200 GMT from what was apparently associated with a storm area that produced severe weather near Seminole, Oklahoma, about 1½ hours later. Activity from this storm and other local thunderstorms was relatively low, characterized by bursts of atmospherics every minute or so producing occasional spikes of high pulse rates. Although a line of thunderstorms formed northwest of Norman, these were not very active and soon dissipated. Activity continued to decrease after about 2400 GMT and observations were terminated at 0320, April 17.

An enhancement in rate activity using slow time constants was observed between about 2320 and 2335 GMT as shown in figure 5. This is not very noticeable at the lower frequencies, but channels 18, 24, 28, 31 and 32 clearly show an increase in the number of rate bursts. The rates, or perhaps the number of atmospherics from each lightning discharge producing these bursts, are somewhat less than what seems to be a general background activity of a few large rate discharges occurring throughout the time period shown in this figure.

No directional data were recorded during this period. Visual observations of the wideband DF, however, indicated the greatest activity was from almost due east. The potential gradient record, channel 38, shows only a few very small deflections ≤ 25 volts

around 2320 GMT, indicating that the thunderstorm producing the few rate bursts associated with these deflections was at least 35 km from Norman, and was decreasing in activity. The enhancement in activity initially referred to does not seem to be associated with this relatively near thunderstorm area. It will later be shown that this type of enhancement is not characteristic of the declining period of a thunderstorm. This gives more weight, therefore, to the probability that the equipment responded primarily to radiation from greater range than the more local activity

A more detailed presentation of some channels of data around 2327-28 GMT is shown in figure 6. There is little correlation between the data in the bottom 4 or 5 channels and the data in the top two-thirds of the figure, i.e., the lower frequency and smaller threshold channels. The data shown in channels 18, 24, and 28, especially, are very interesting in that repetitive bursts of activity every 6 seconds or so is indicated by the rate spikes.

Original reports indicated a tornado had touched down about 5 km NW of Seminole, Oklahoma, at 2330 GMT. This was later downgraded to a severe windstorm by the National Severe Storms Forecast Center in Kansas City. A radar frame showing the extent of precipitation at 2318 GMT is shown in figure 7. North is along the straight arrow pointing up in the upper center of the figure and range from NSSL is given in nautical miles (n mi) which is also the format for all subsequent radar frame presentations. The arrow pointing to an area due east of NSSL indicates the location of the severe weather.

More detailed rate data on an expanded time base are presented for comparisons with figure 6. Data recorded about 10 minutes after the time at the right of figure 5 are shown in figure 8. Tape recorder induced noise that was just noticeable in figure 6 had become quite objectionable on channels 11-16 in figure 8. There is an obvious reduction in electrical activity shown in figure 8 relative to figure 6. Channels 10, 14, and 25 contained no data and are not shown in figure 8, and channels 18, 24, and 28 show a marked decrease in the number of lightning discharges.

Figure 9 shows data recorded at 0142 GMT on April 17. A further reduction in thunderstorm activity can be inferred by comparing figure 9 with figure 8. No rate data were obtained for channels 24, 25, and 28. Channels 26 and 27 were in service at this time and channel 26 data are presented but no pulses exceeded the channel 27 threshold and are therefore not presented. The small spikes on channels 6-10 were caused by the tape recorder and these will be seen also in subsequent figures.

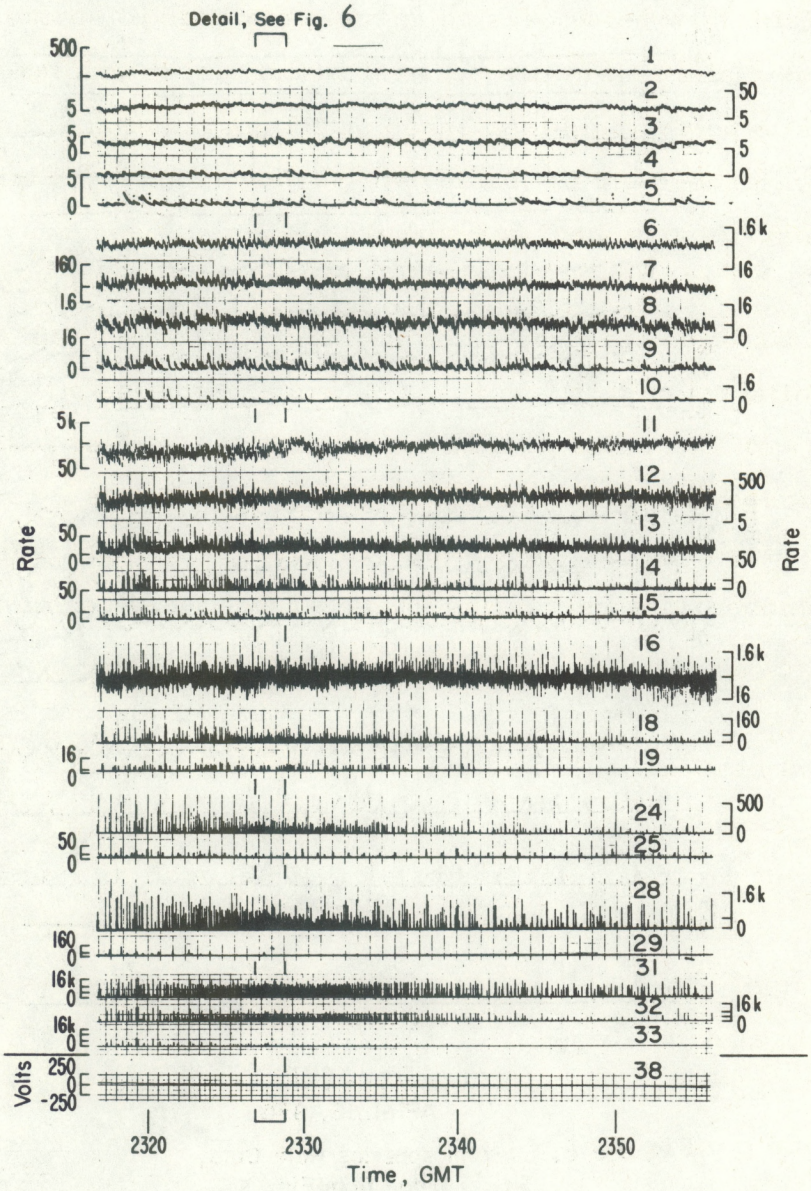

Figure 5. Atmospherics Rate Data

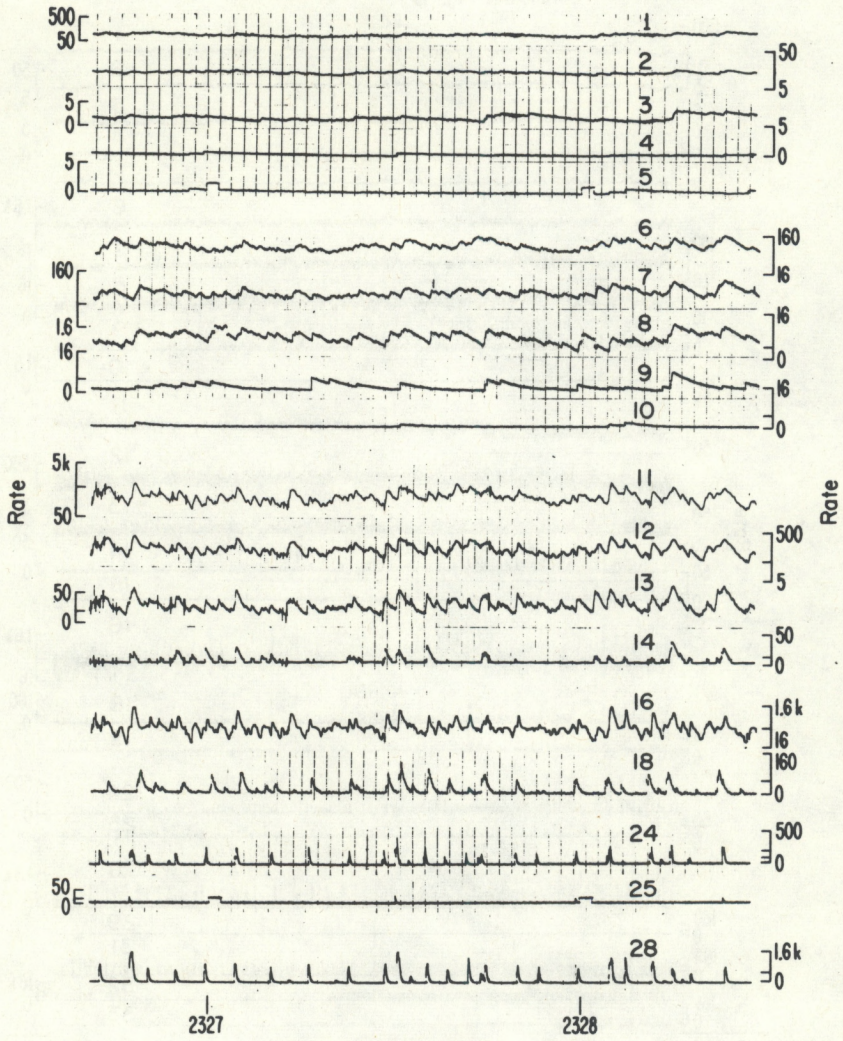

Figure 6. Atmospherics Rate Data, Detail from Fig. 5.

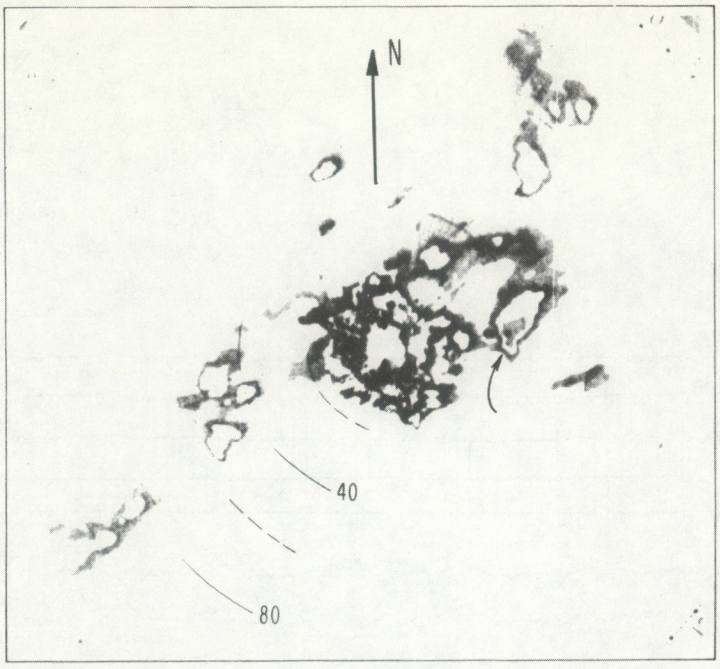

Figure 7. Radar Frame N°. 7480
April 16, 1970 2318 GMT

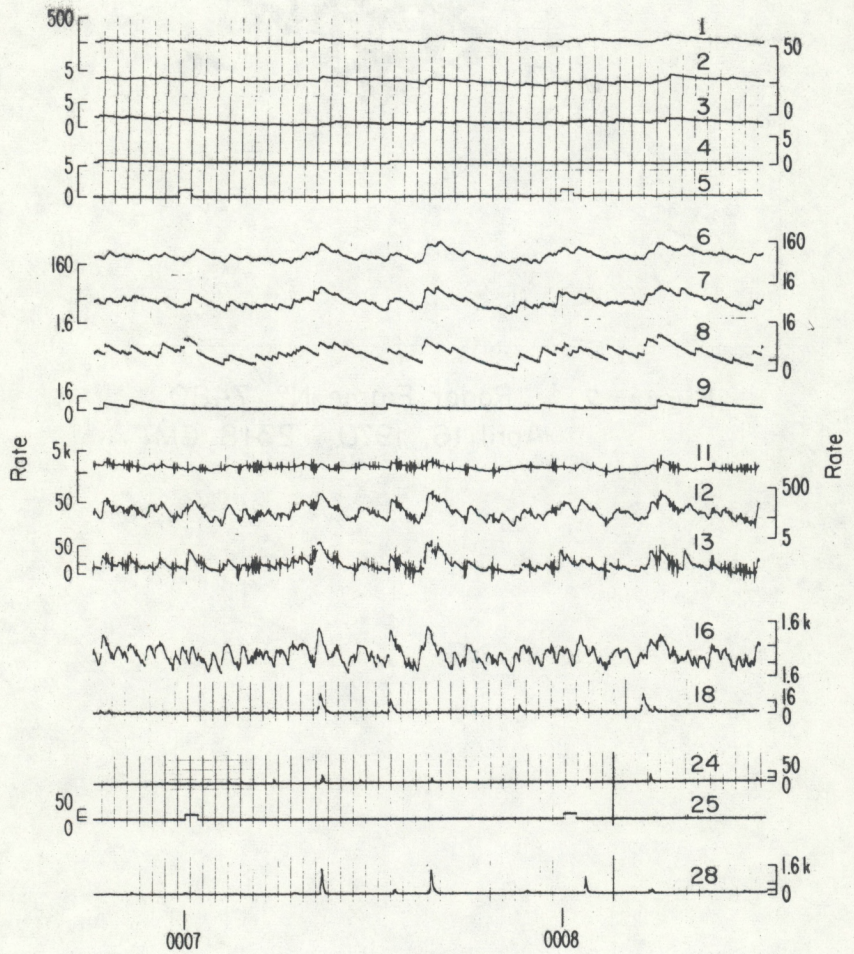

Figure 8. Atmospherics Rate Data, Expanded

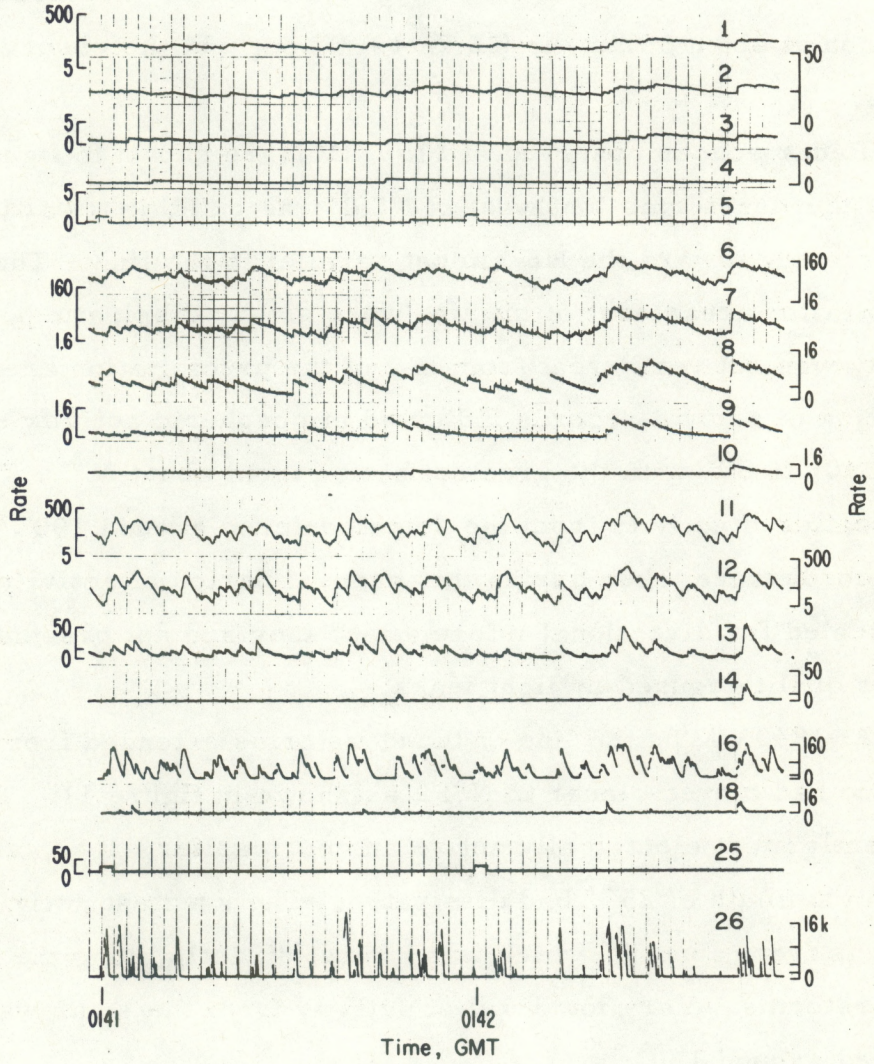

Figure 9. Atmospherics Rate Data, Expanded

3.2 Funnel and Tornado Activity on April 18-19

Thunderstorm activity began to build up by midmorning. Observations started at 1715 GMT and continued through 0225 GMT April 19. Radar indicated precipitation moving in a generally northeasterly direction at about 55 km/hr (30 knots) throughout the observation period.

Radar echoes observed at 1750 GMT are shown in figure 10. The line of thunderstorms just west of NSSL was building toward the SSW while moving toward the NE almost parallel to the line. The large precipitation areas east of the line were slowly dissipating. Electrical activity was not very great from any of the precipitation areas. Direction of arrival records indicated atmospheric activity extended from 340° to 80° with the greatest action from about 25°. There was also scattered activity from the south centered around 190°. Although DF records were taken during this general period of activity, and have been scaled for directional information, they are not presented because of poor quality caused by light leaks.

At 1840 GMT, the line of thunderstorms extended from NNE to SSW and had moved closer to NSSL as shown in figure 11. The area apparently most electrically active an hour earlier, i.e., atmospherics from an azimuth of 25°, had dissipated. The greatest activity at this time was from about 5° which was almost directly along the line of thunderstorms. Very low level of activity from the south was also centered around 160°.

By 1954 GMT the line of thunderstorms had moved east of Norman although the line was very unorganized near NSSL as shown in figure 12. A funnel was reported at 1945 in an area indicated about 95 km north of NSSL by the arrow.

Figure 13 shows the line at 2225 GMT had become better organized and had moved toward the east as the individual storms continued to move northeastward. A tornado was reported at 2225 GMT; later changed to 2210 GMT by NSSFC; about 80 km southeast of NSSL as indicated by the arrow. The nearest thunderstorm was about 40 km east of NSSL at 2200 GMT. Atmospheric activities from this and other storms along the line were relatively low and continued to decrease until observations ceased. Thus, no enhancement in atmospheric rates were recorded during this reported tornado. Other tornadoes or funnels were reported in northeastern Oklahoma near Checotah and Tulsa between 0000 and 0100 GMT April 19. No enhanced activity was observed from these which was to be expected because they were beyond the experimental range of the observations.

Atmospheric rate data (slow time constant) between 1916 and 1956 GMT are shown in figure 14. Activity is relatively low around 1920 GMT but shows a definite increase in rates at about 1935 GMT. A broad peak in activity is centered near 1947 after which the rate data show a decrease. Although not presented, electrical activity continued to decrease until it approached a level equal to the activity around 1920 GMT.

There was a local thunderstorm only a few kilometers east of NSSL at 1950 GMT as indicated by the large deflections on the potential gradient data at the bottom of figure 14. Lightning discharges from this storm produced essentially all the rate data shown on channels 25, 29, and 33, and produced some of the larger spikes shown on the other channels. Thunder was heard at NSSL from the discharge that produced the rate data spikes that are observed on all channels just prior to 1950. It might be mistakenly assumed that all the enhanced rate data resulted

from the nearby storm. However, very little radio emission was indicated from the direction of this storm from the DF records. The greatest concentration of activity was from a direction narrowly centered around 12°. This corresponds to the direction of the tornado funnel indicated in figure 12, which was perhaps the true source region of the enhanced atmospheric rates shown in figure 14.

Two selected times for a detail look at the enhanced period of data in figure 14 were chosen. The first selection near 1947 GMT, shown in figure 15, was just at the peak of the enhanced activity, and the second selection at 1951 GMT, in figure 16, was slightly after the peak. Focusing our attention primarily on the higher frequency channels in the bottom half of these figures, we find that the bursts of atmospherics producing these spikes in the rate data are closely spaced in time. In figure 15, the bursts are shown to have occurred about once per second, while in figure 16, the bursts occurred less frequently at about every $1\frac{1}{2}$ second. The peak rate of the individual burst tended to be about the same value as most of the other bursts in each channel in both figures. This characteristic was also observed for the April 16 data shown in figure 6. The occasionally large rate spikes were produced by the lightning discharges in the nearby storm.

The data (slow time constant) observed near the time of the radar frame shown in figure 10 are presented in figure 17. The atmospherics received during this period were indicative of low electrical activity even though a number of thunderstorms were very near NSSL. The short spikes on channels 11-16 were caused by tape recorder problems and should not be confused with atmospheric rates.

Figures 18 and 19 are presented to give a comparison between fast time constant and slow time constant data recorded during periods

of low activity. These are the figures referred to by the detail brackets in figure 4 which presented only channels 11-15. Also, channels 11-15 used as samples in figure 3 are presented in figure 19 after spacing the data closer together to conserve space and aid the eye in following various details.

Nearby thunderstorm activity not associated with severe weather was similar to the data shown in figures 17, 18, and 19. The general characteristics for non-severe activity observed here was for a few bursts per minute to activate the higher-frequency and larger-amplitude channels. These data should be contrasted with those presented in figures 15 and 16 which were perhaps representative of rate data characteristics for severe weather.

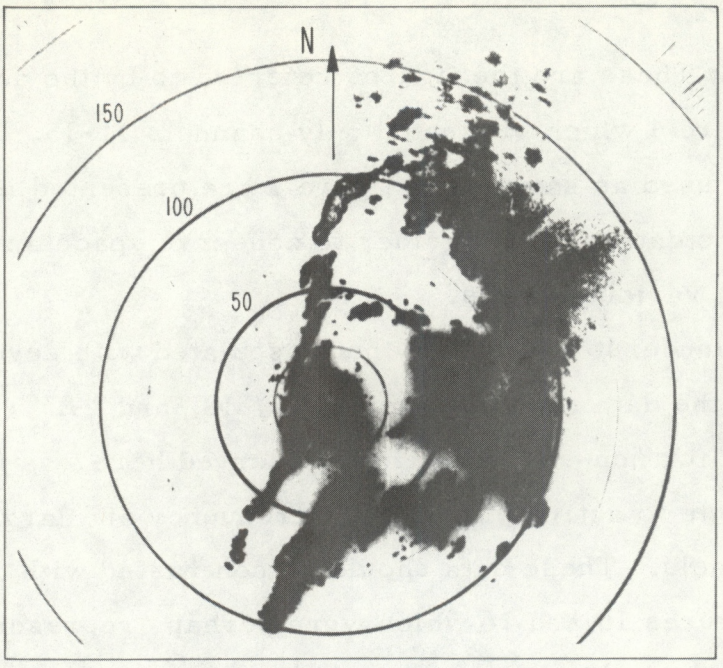

Figure 10. Radar Frame N° 1881
April 18, 1970 1750 GMT

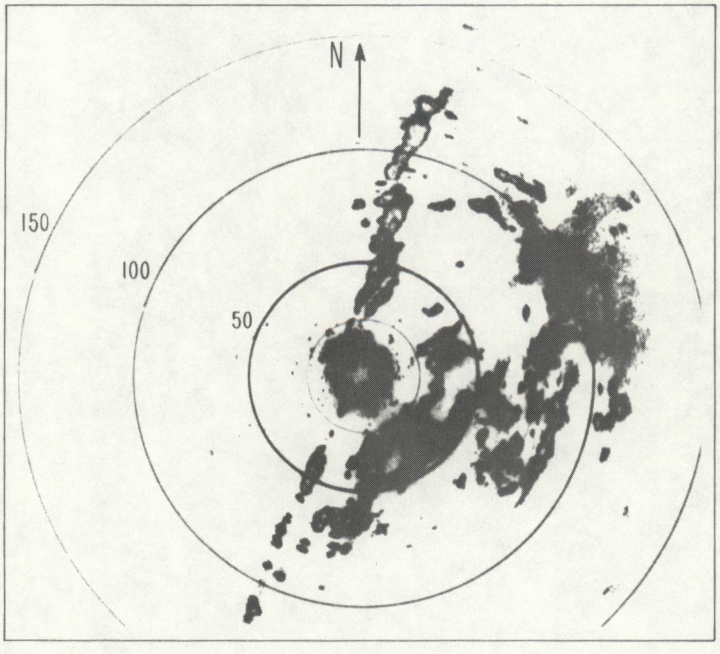

Figure 11. Radar Frame N° 2031
April 18, 1970 1840 GMT

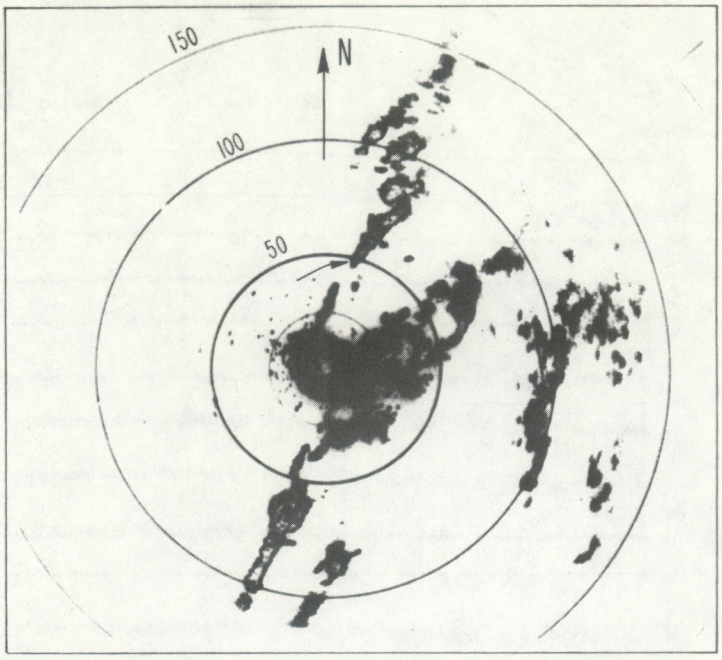

Figure 12. Radar Frame N°. 2253
April 18, 1970 1954 GMT

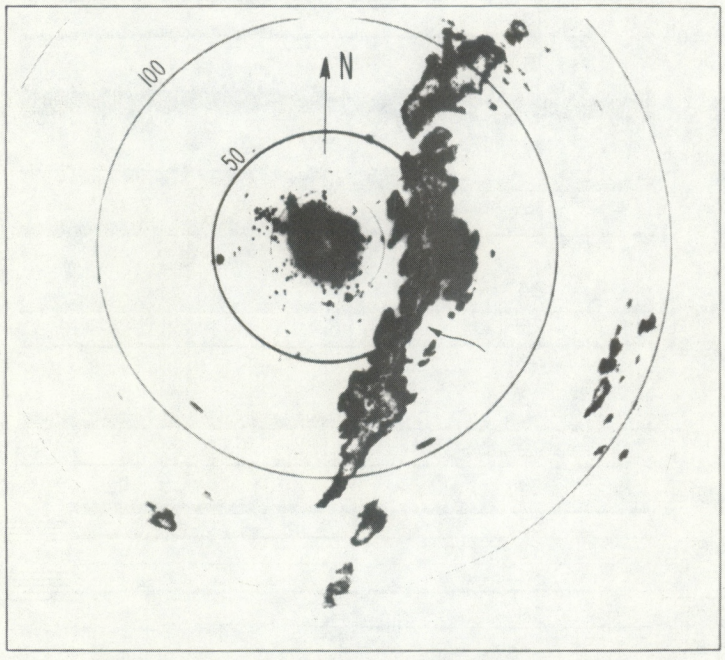

Figure 13. Radar Frame N°. 2697
April 18, 1970 2225 GMT

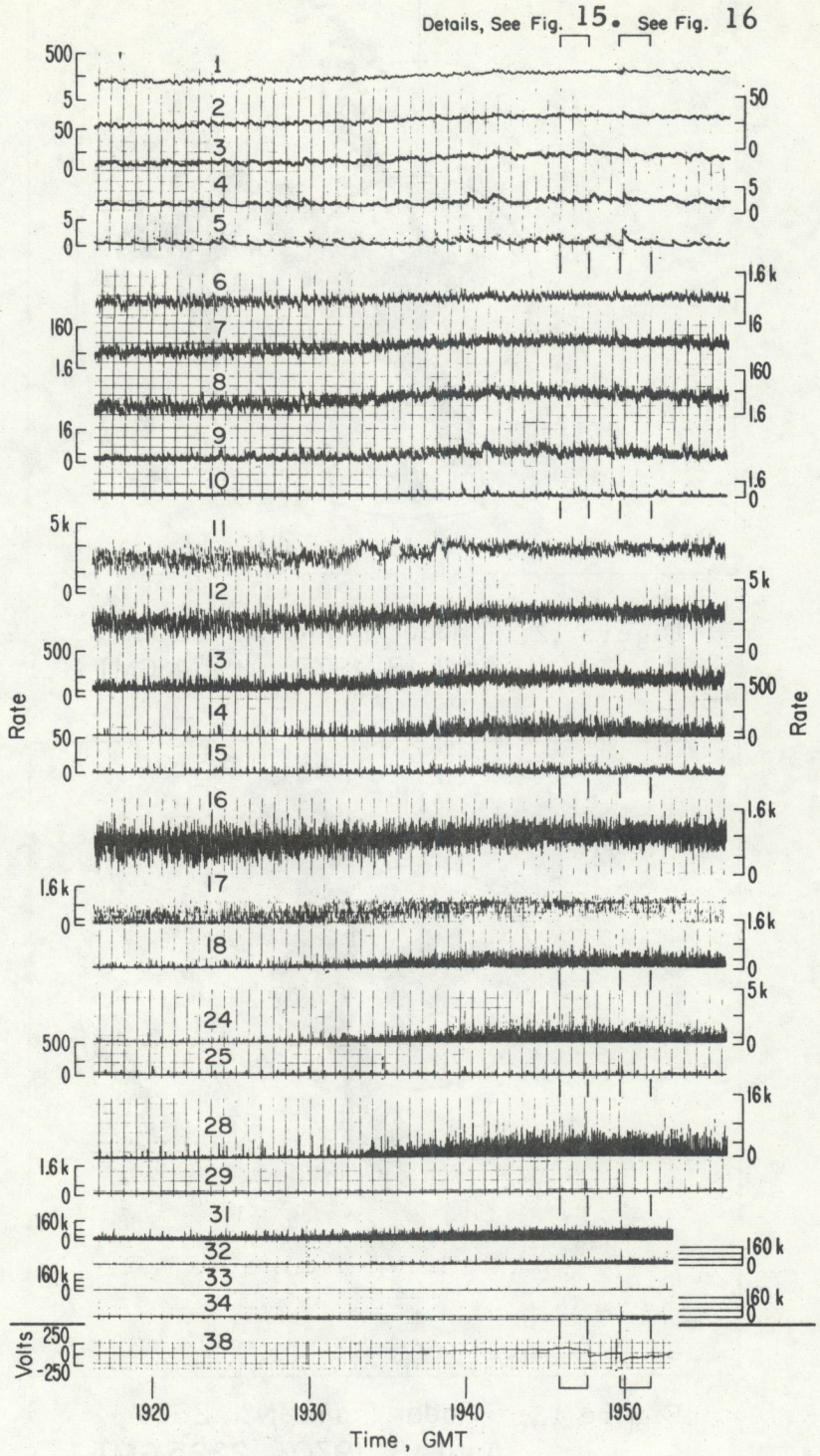

Figure 14. Atmospherics Rate Data

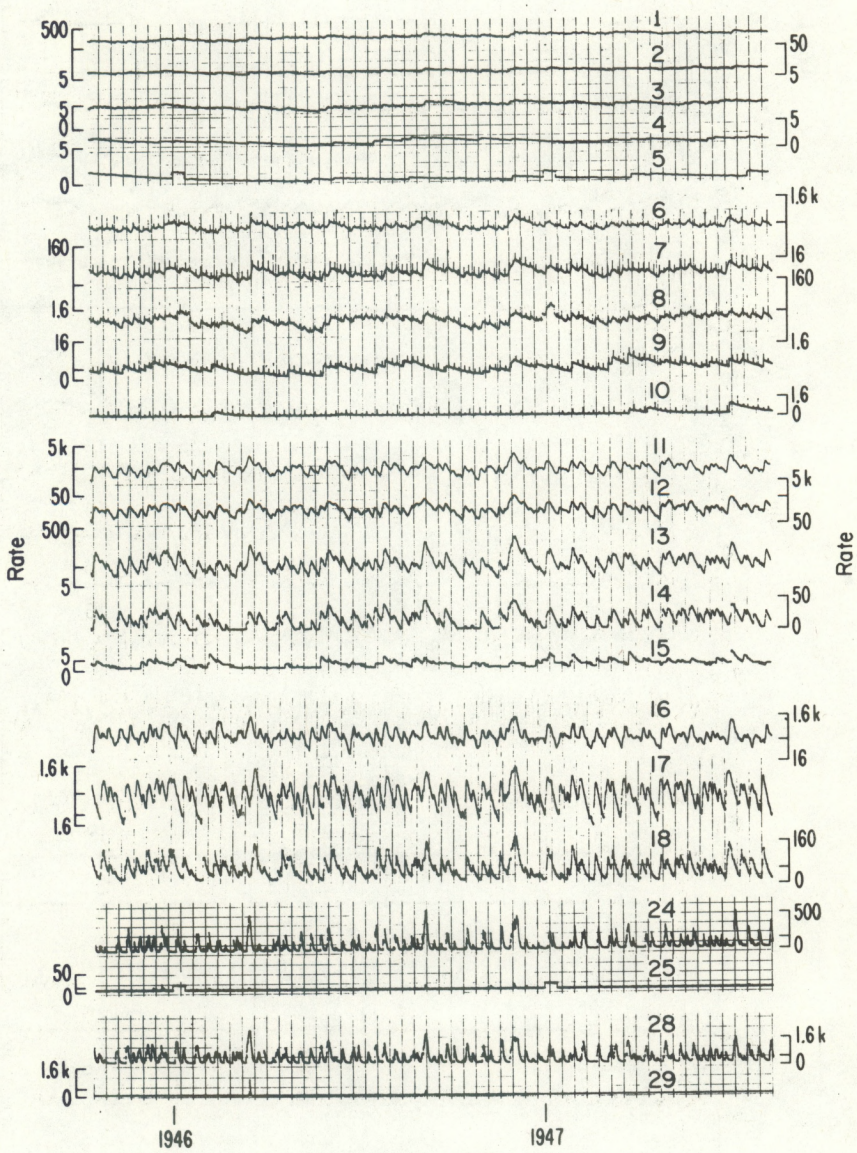

Figure 15. Atmospherics Rate Data, Detail from Fig. 14.

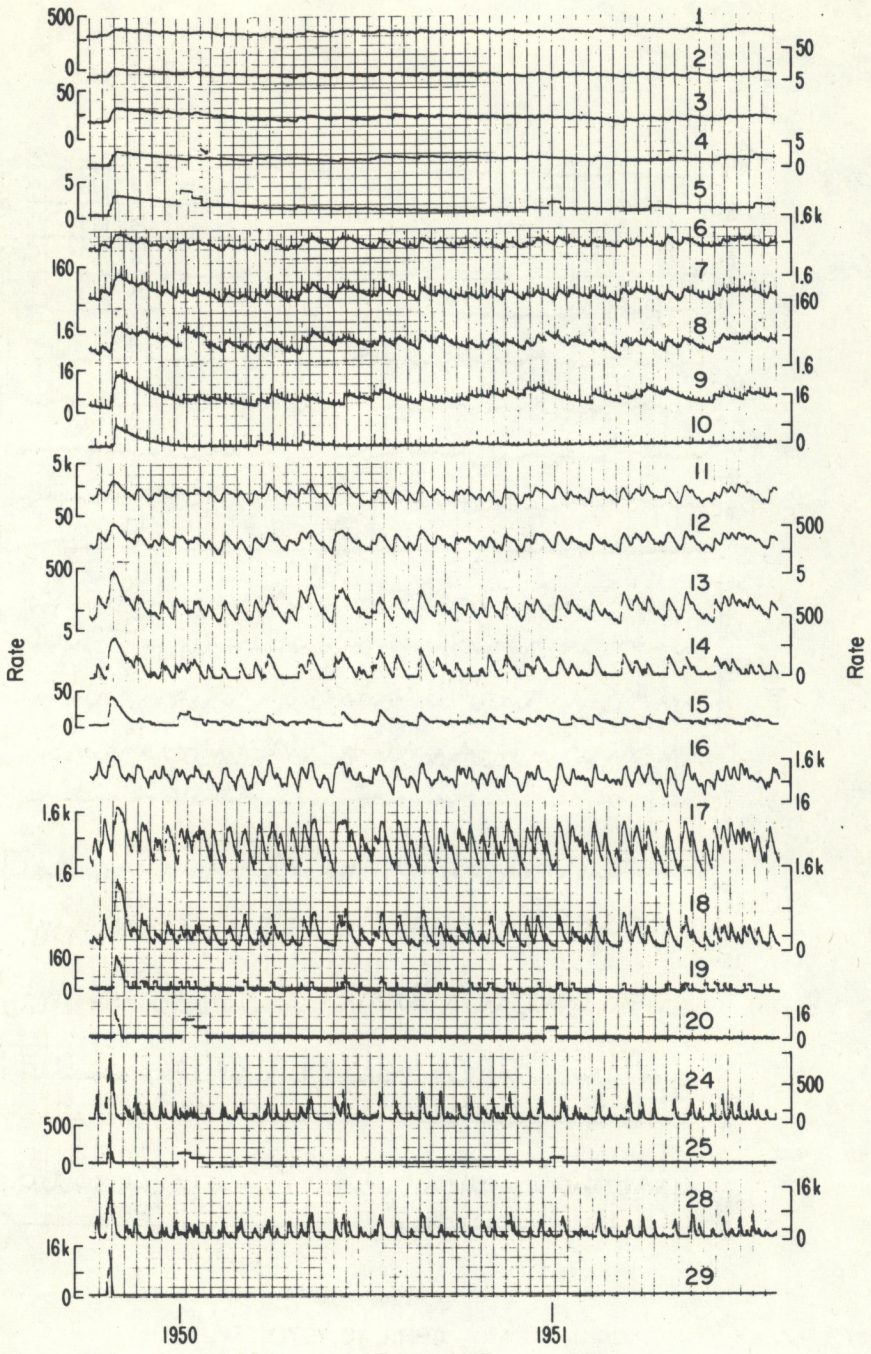

Figure 16. Atmospherics Rate Data, Detail from Fig. 14.

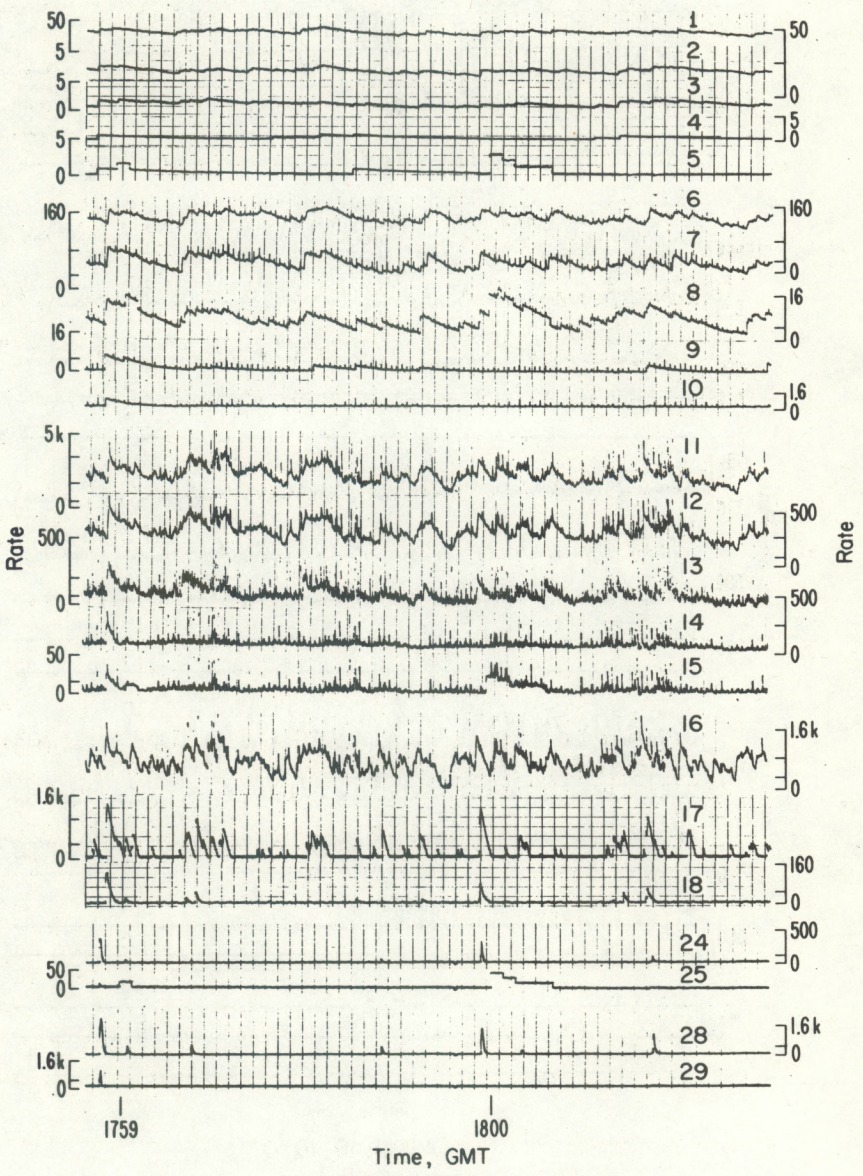

Figure 17. Atmospherics Rate Data, Expanded

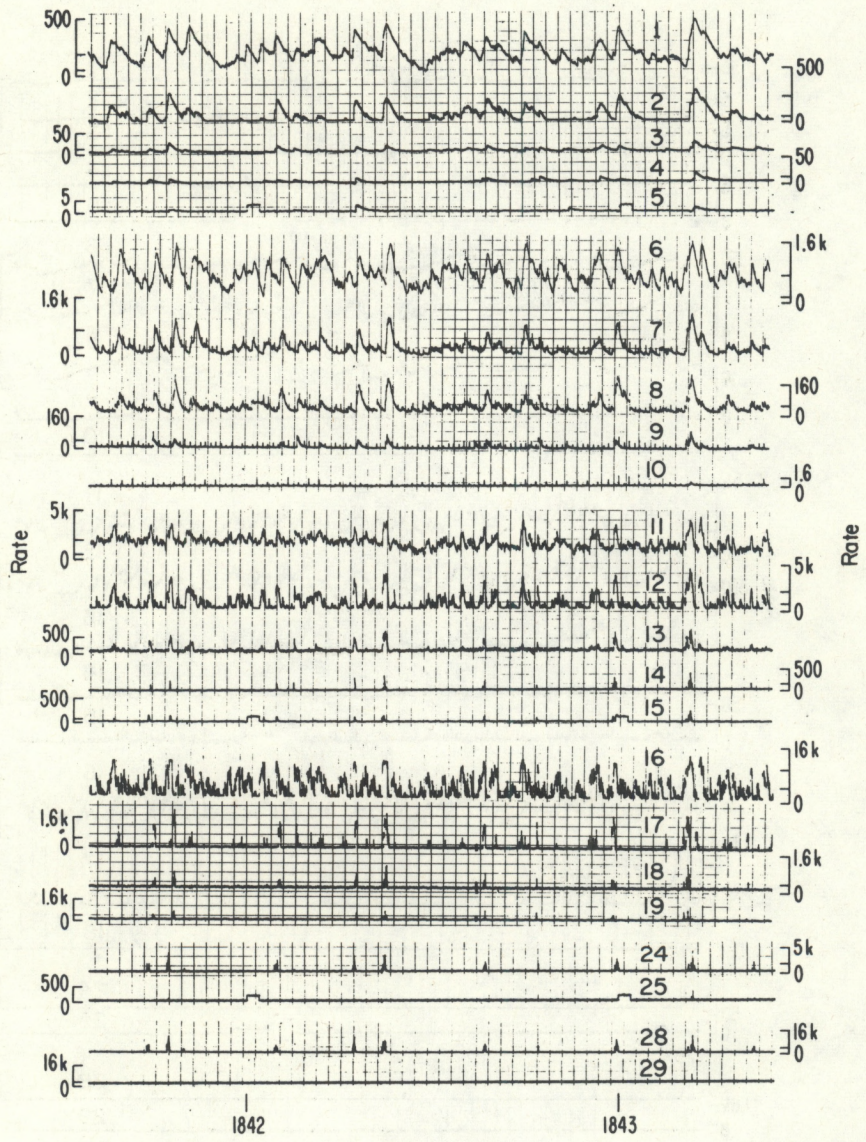

APRIL 18, 1970

Figure 18. Atmospherics Rate Data, Expanded
(Detail from Fig. 4)

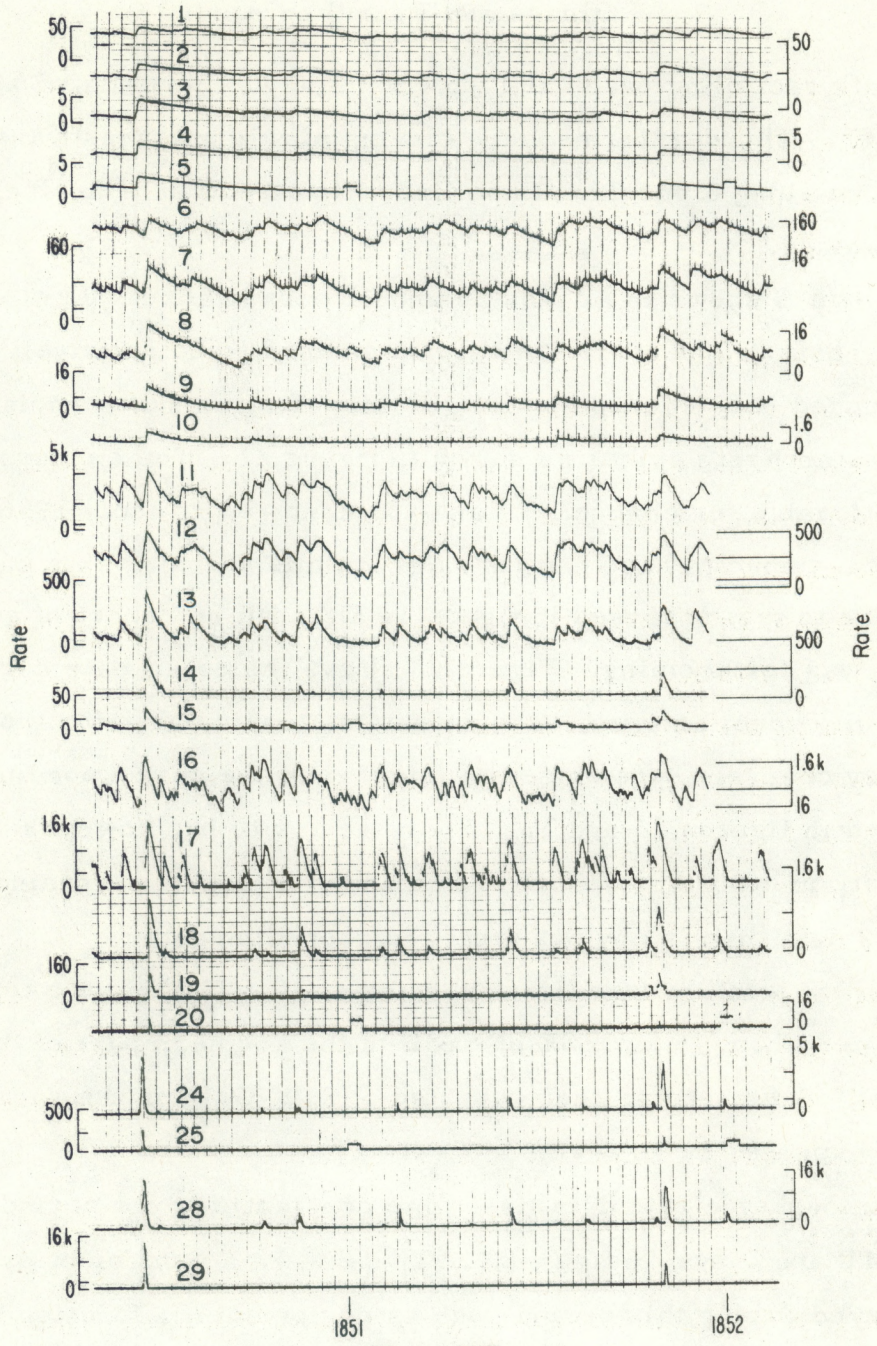

Figure 19. Atmospherics Rate Data, Expanded
(Detail from Fig. 4)

3.3 Storms and Funnel on April 23

Data recording began at 1725 GMT and was terminated at 2400 GMT. Thunderstorms were moving slowly northeastward during this period along a poorly defined line. No direction of arrival data were obtained.

Storm A shown in figures 20 and 21 passed about 20 km south of NSSL at about 2000 GMT. This storm seemed to be relatively inactive and produced only a few potential gradient changes and associated (slow time constant) rate spikes as shown in figure 22. The enhanced activity, most noticeable for channels 24 and 28, centered at about 1956-57 GMT must be assumed to have had its origin in this storm. This enhancement is similar to that observed in figure 14 although no report of severe weather was forthcoming. Figure 23 shows the detail data during the time of maximum activity. The rate data, particularly for the higher frequency channels, are somewhat similar to the corresponding data presented in figures 15 and 16. There seems to be, however, greater variability in peak atmospheric rates and in burst time spacing in the figure 23 data than is obvious from the preceding data.

Severe weather was first reported at 2045 GMT in the form of hail located about 75 km ESE of NSSL in the southern part of thunderstorm B. A funnel was then reported at 2100 GMT in the same general area as indicated by an arrow in figure 21.

Atmospheric rate data (fast time constant) for the period 2031-2114 GMT are shown in figure 24. There were a number of problems encountered during this period such as equipment malfunction for channels 1-5, disruption of power to the rate equipment caused by an open breaker near 2045 GMT, and the recorder for channels 24-29 was

out of tape between 2056-2108 GMT. Atmospheric rates were evidently enhanced around 2050 GMT, although a greater elevation in rates occurred between 2100-2110 GMT on channels 31 and 32.

Detail data centered near 2050 GMT are presented in figure 25. The frequency of bursts, most readily seen in channels 24 and 28, was high but the peak rate values and the burst spacings were quite variable. Unfortunately, there is no way to determine the source location for this activity.

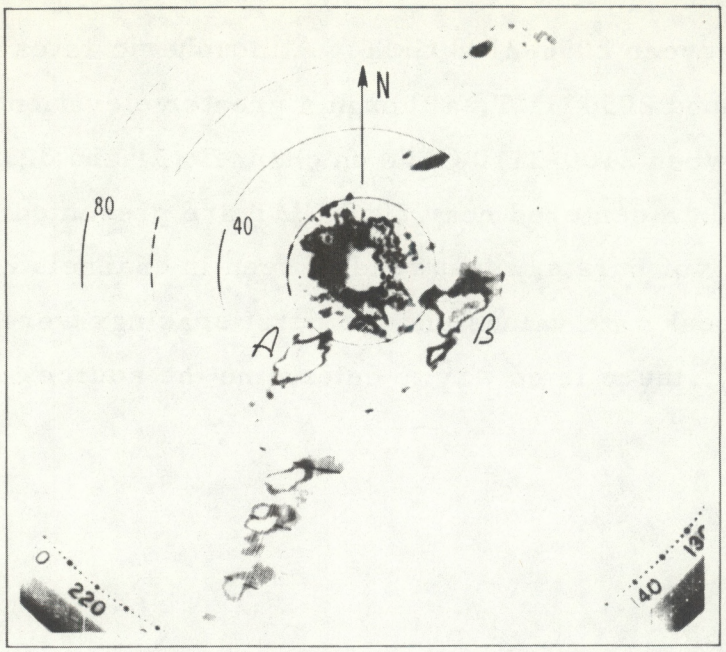

Figure 20. Radar Frame N° 3117
April 23, 1970 1921 GMT

Figure 21. Radar Frame N° 3354
April 23, 1970 2045 GMT

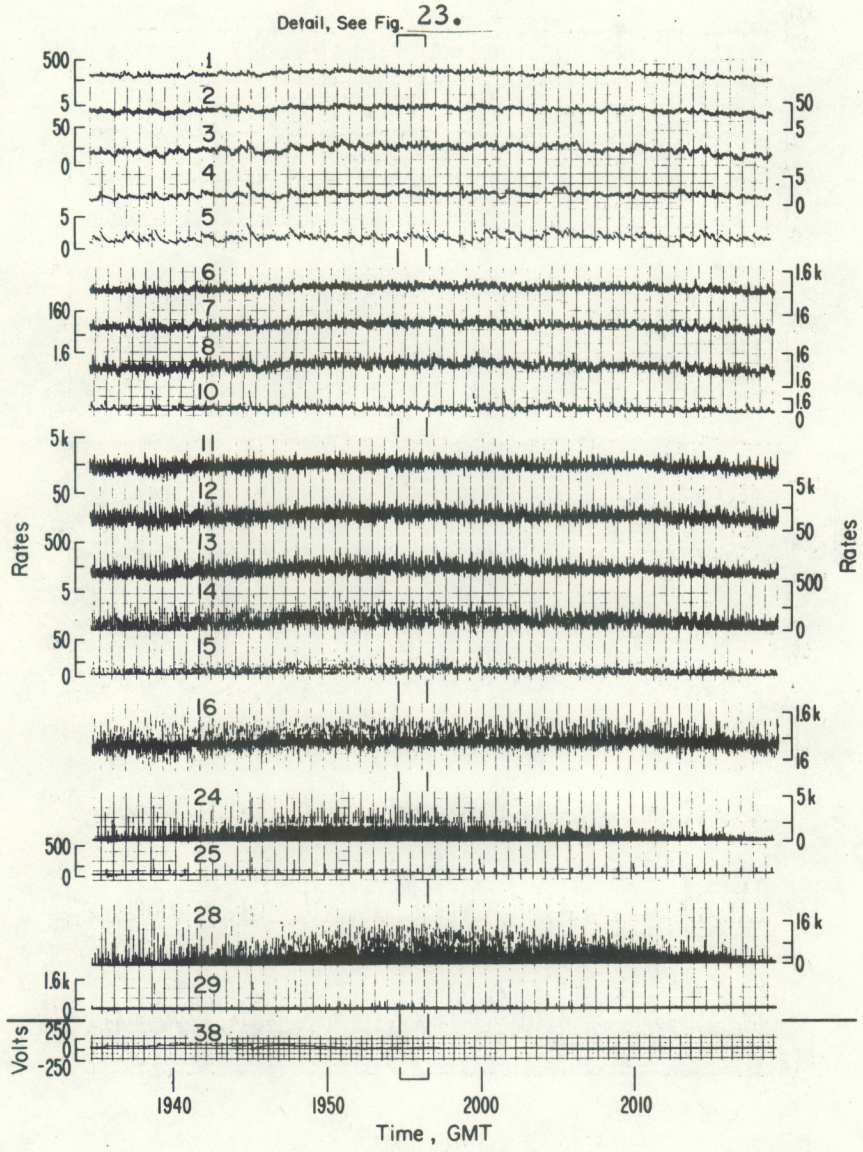

Figure 22. Atmospherics Rate Data

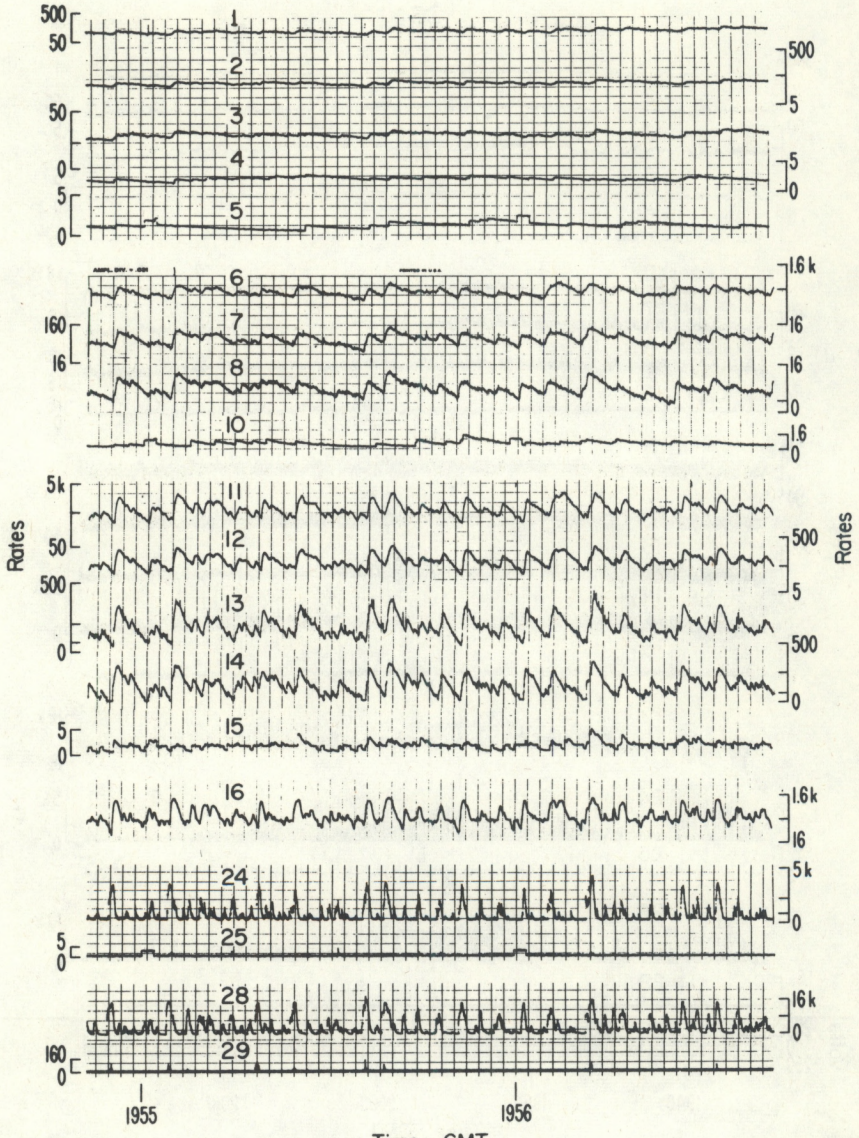

Figure 23. Atmospherics Rate Data, Detail from Fig. 22.

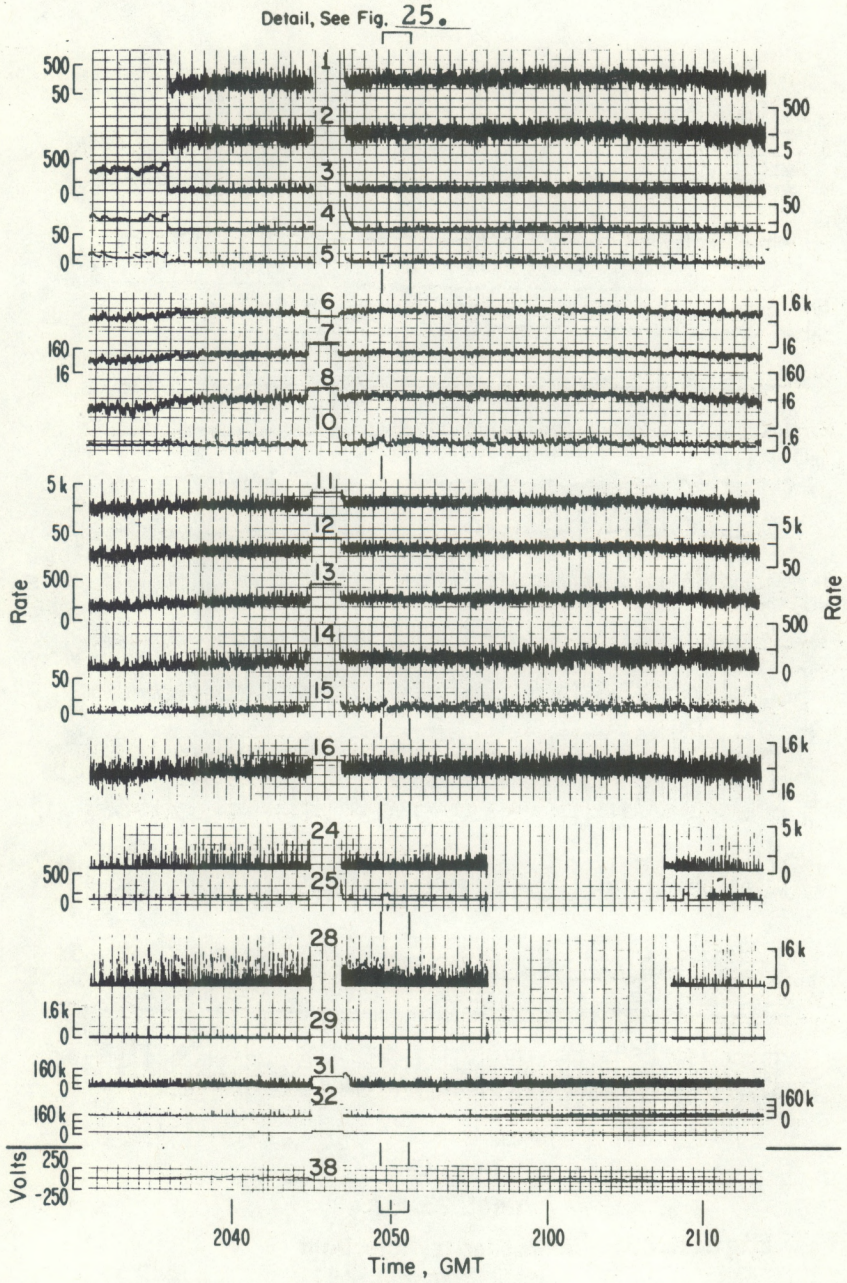

Figure 24. Atmospherics Rate Data

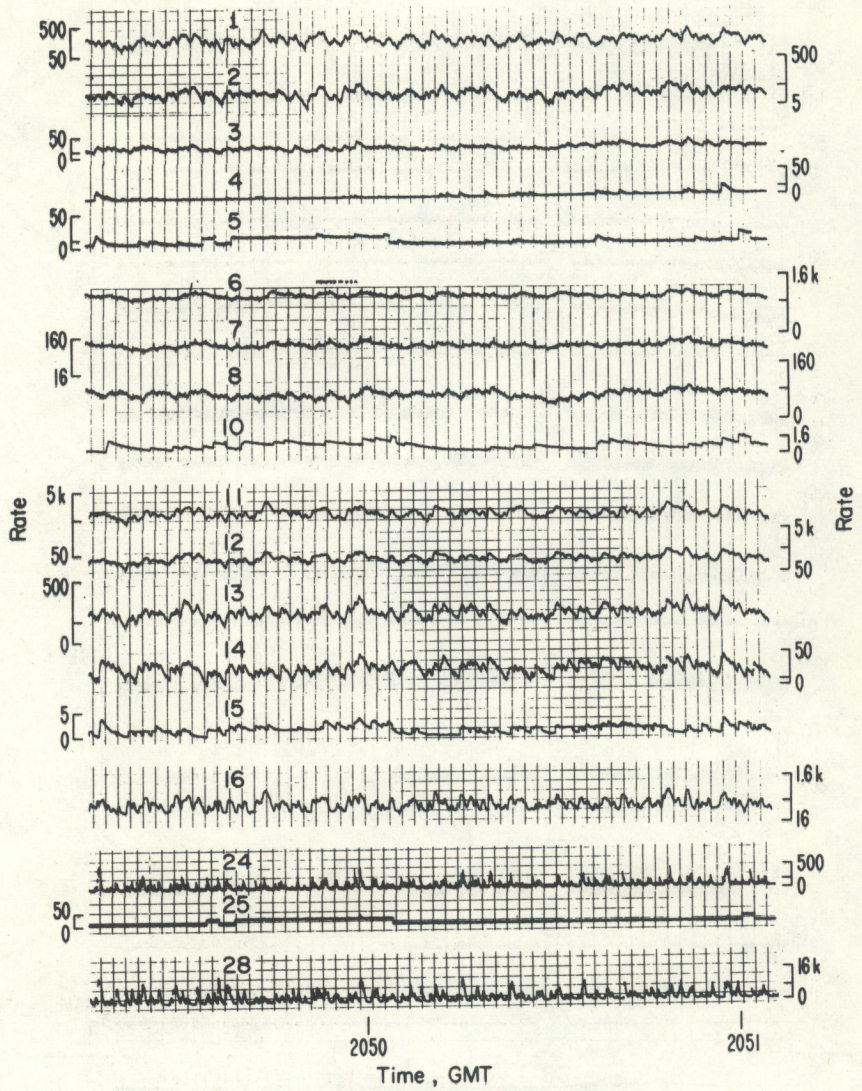

Figure 25. Atmospherics Rate Data, Detail from Fig. 24.

3.4 The April 25 Thunderstorm

A very large thunderstorm region developed southeast of NSSL around local noon on this date. Observations began about 1810 GMT and ended about 2030 GMT. The radar returns at 2000 GMT are presented in figure 26. A maximum in electrical activity from a SSE direction indicated by DF was undoubtedly associated with the region of maximum precipitation shown in the radar picture as the enclosed light shaded area.

No severe weather was associated with this storm, but slow time constant rate data on an expanded time base is presented in figure 27. The very high peak rates of long duration occurring about once each minute seem to be characteristic of large mature storms during the decaying period. Other examples of this will be presented later.

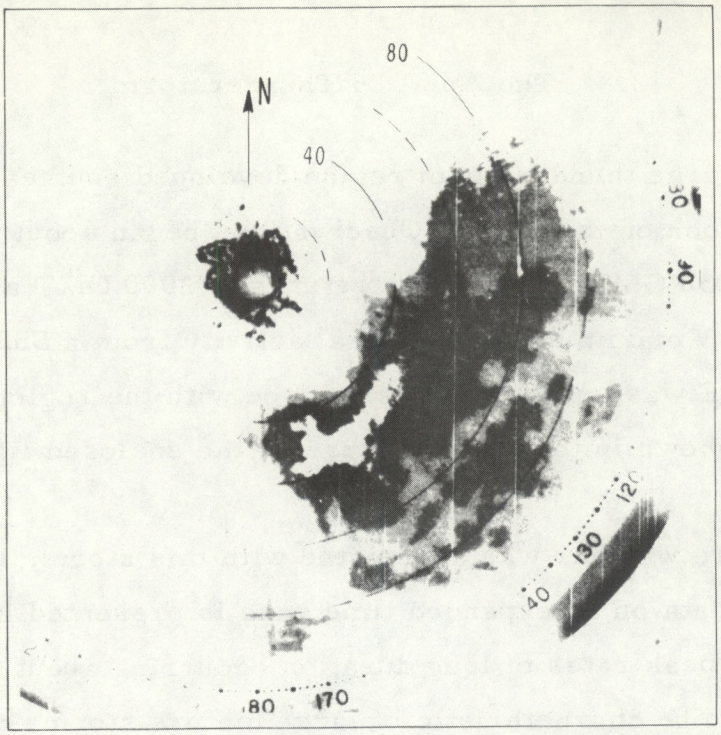

Figure 26. Radar Frame Nº 5231
April 25, 1970 2000 GMT

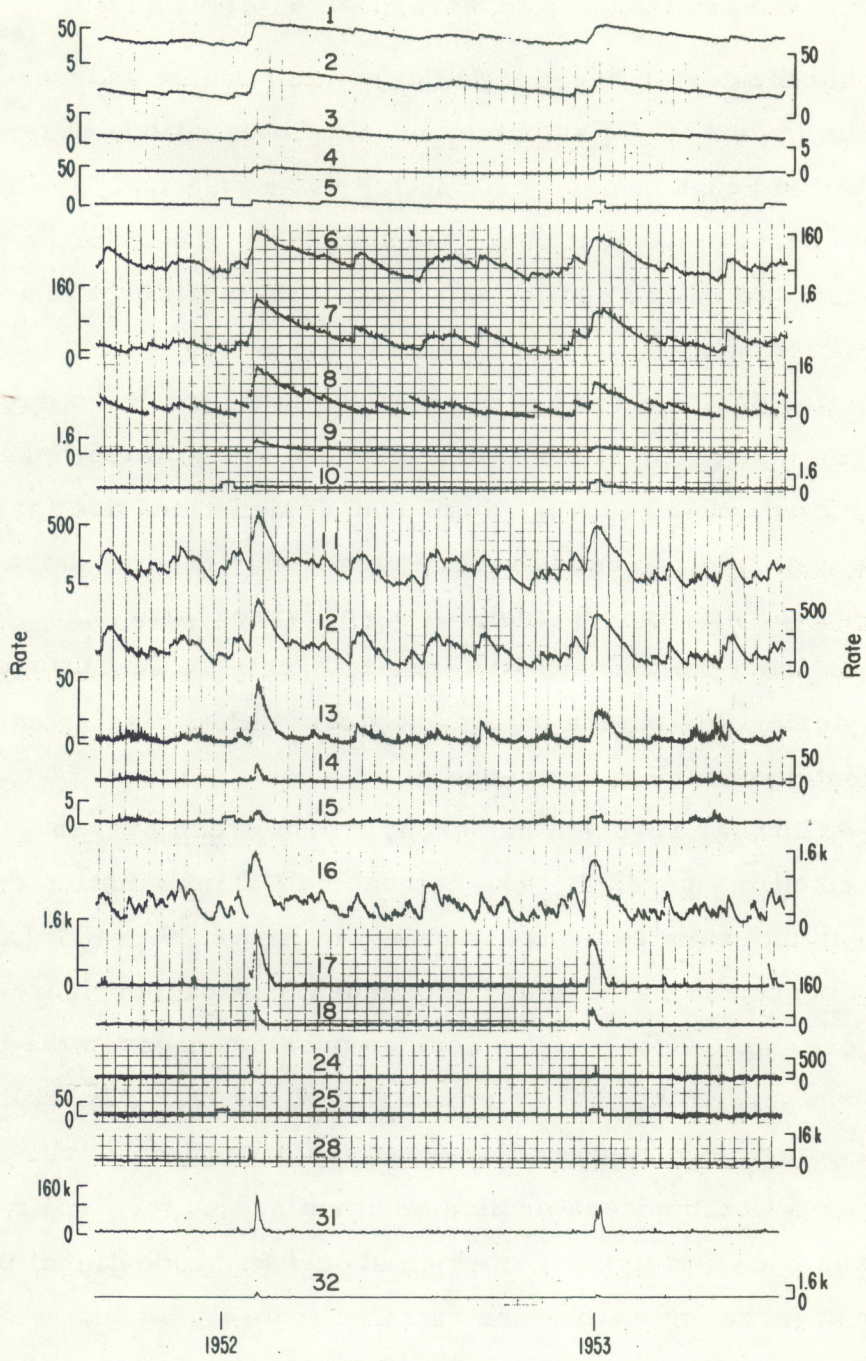

APRIL 25, 1970

Figure 27. Atmospherics Rate Data, Expanded

3.5 Severe Storms and Tornadoes on April 29-30

Thunderstorms began to build by midmorning and were numerous in central Oklahoma by noon. Observations began at 1900 GMT although atmospheric activity was relatively low at that time. General movement of the thunderstorm areas during the period covered in this section was toward the northeast at about 75 km/hr (40 knots).

Letter designations, such as shown in figure 28, correspond to the storms identified by NSSL in the Preliminary Review of Storm Data for April 29-30, 1970. Numbered designations are for other active thunderstorm areas that are identifiable from radar and DF data. These designations assist in identifying storm areas for reference from the text and in following each area in subsequent figures during this period until each storm either dissipated or moved outside of the radar range.

NSSL radar revealed numerous storm areas present at 2220 GMT as presented in figure 28. The companion DF information contained in a 17-minute time exposure is shown in figure 29. The times for the data presented in these and subsequent companion figures do not always overlap. This is not a serious problem because the primary interest in presenting these companion figures is to reveal the general correlation between the radar and direction of arrival data. The more active thunderstorms as determined by the density of the DF traces shown in figure 29; which should be proportional to the number of larger atmospherics radiated from each area; were 2, 3, 6 and C. Storm 1 was very small; 4 and 5 were not

recognizably separated on the DF although 4 was the more active of the pair; and 7, B, 8 and 9 were essentially merged into a wide angle of activity. It should be noted that storm A was not electrically active at this time because no atmospherics indicated by the DF display can be associated with it.

Figures 30 and 31 show the radar and DF situations at 0104 GMT April 30. Unfortunately, the center spot intensity for the DF was too bright and fogged the film obscurring the low amplitude atmospherics. Many of the thunderstorms previously shown had died out by this time. Storm areas 5 and 6 were merged; C was still very active; B had increased to the most active storm in the line of thunderstorms in which it was associated; and 9 remained active.

The elliptical or loopy traces in the DF presentation were produced by a few atmospherics from storm A which was passing over NSSL at this time. Loopyness such as this can be caused by vertical and horizontal magnetic field components of a signal arriving at high elevation angles and also by the induction field component of a signal from nearby or local lightning strokes.

The situation around 0200 GMT is shown in figures 32 and 33. A light leak caused some fogging on the DF film. At this time, C had passed over NSSL and had remained inactive. Storms 5 and 6 remained merged and were still active. A scattered storm area labeled 10 was building and producing some atmospherics. Area 11 was electrically active but was just beginning to produce radar returns. Storm system E was active and moving closer to NSSL. Storm D was not active. Storms B and 9 were decreasing in activity and moving out of the area of interest.

Storm system E continued to move closer to NSSL as shown in figure 34 and was highly active during the DF time exposure period as indicated in figure 35. Storm C had almost dissipated and storms 5 and 6 had moved far to the northeast. Area 10 had become quite active. The DF display shows distortion in the larger amplitude signals from area 10 because of limitations in the horizontal amplifiers of the oscilloscope. Storms 11 and 14 seemed to be producing only occasional large atmospherics. A storm region marked 15 was not very active. There was considerable widespread activity from directions of 245°-280° from scattered thunderstorms west of NSSL. Storm F appeared in the southwest but its electrical activity was masked by storm E.

The electrical activity from nearby thunderstorms after 0345 GMT had increased to the level that the presentation of the time integrated DF data would not be profitable for recognizing discrete directions from which atmospherics were arriving and for following active areas.

Figure 36 shows that the leading portion of storm area E was within the ground clutter radar returns. This storm was close enough to visually observe lightning discharges. Although the DF observations are not presented, examination of the DF data indicated that storm areas 15 and 10 were still active while storm 14 remained inactive. Activity from storm F remained masked by storm E.

Storms E and 15 had formed a short line and the southern part of storm E was centered just west of NSSL at about 0450 GMT as shown in figure 37. Atmospheric activity extended from about 220° through north to about 30°. The greatest concentration of the activity was from around 240° (the southern part of storm E), 340° through 360° (the northern part of storm E), and from about 25° which

indicated storm 15 was still active. There was also isolated activity from storm 10 at an azimuth of 60°. Activity from storm F and other scattered thunderstorms west and northwest of NSSL could not be identified through the atmospherics originating from the southern portions of storm E. It should be noticed that storm G had just come into the radar picture in the southwest at this time.

Atmospheric activity completely filled the oscilloscope display from an azimuth of 240° through north to about 30° at 0545 GMT. The location of storms 15, E, F, and G at this time are shown in figure 38. The southern part of storm E was beginning to break away from the Norman area and move toward the northeast. Storm F was centered about 90 km (50 n mi) west of NSSL and storm G was moving along the same path that F had followed.

The radar frame at about 0700 GMT presented in figure 39 shows storm E moving well off toward the northeast. Storm G had greatly intensified and had moved in very close behind storm F. Another radar presentation taken at 0703 GMT is shown in figure 40. This was approximately the time when the first Oklahoma City tornado was reported to have passed through the far northwestern section of that city, associated with the southern appendage of storm F. This would place the tornado in the direction of about 335° at 42 km (23 n mi).

Direction of arrival data obtained during this period are shown in figure 41. This group of six exposures were similar to the DF data previously shown but were for a time period of one second each compared to several minutes for the other data. The camera shutter was open continuously and the film was advanced between frames at a transport speed of 25 cm/s which required only a small fraction of a second. Film movement was actually vertical and the time between exposures moved up such that the top of the first frame is approximately

the same time as the bottom of the second frame, and so on. Individual atmospherics that arrived during each film advance was recorded above and below the center of each time exposed frame.

The first 1-second DF display on the left side of figure 41 was taken at 0704 GMT and 1 second, and the last display on the right was taken at 0704 and 6 seconds. Atmospheric activity as indicated by the frames, tended to be more persistent from the directions of about 300° and 340°. There were a few atmospherics from 40°, associated with storm E, and from about 210°, probably from storm 16 that was shown in figure 39. The most active area at this time was the center part of storm G, near the actual placement of that letter in figure 40. The persistent direction of activity seems to agree reasonably well with the approximate location for this first tornado.

The second tornado through the Oklahoma City area between 0720 and 0740 GMT was probably spawning almost due west of NSSL at the time of the radar frame in figure 40. The central part of the storm G complex tended to bow out or rotate about the leading part of the storm as shown in figure 42. The first tornado had evidently dissipated by 0730 GMT and the second tornado was probably located about 31 km (17 n mi) in a direction of about 340° from NSSL. The 1-second directional displays starting at 0733 and 2 seconds, and ending at 0733 and 7 seconds are shown in figure 43. The most persistent direction of arrival was about 340°. Although this was the direction of the tornado at about this time, it was also the direction toward the main central part of storm G which had been consistently active for a longer period of time.

The lower portion of storm G reached NSSL at 0745 and disrupted power to the radar. Power was only momentarily interrupted at the atmospherics site and observations continued until 0830 GMT.

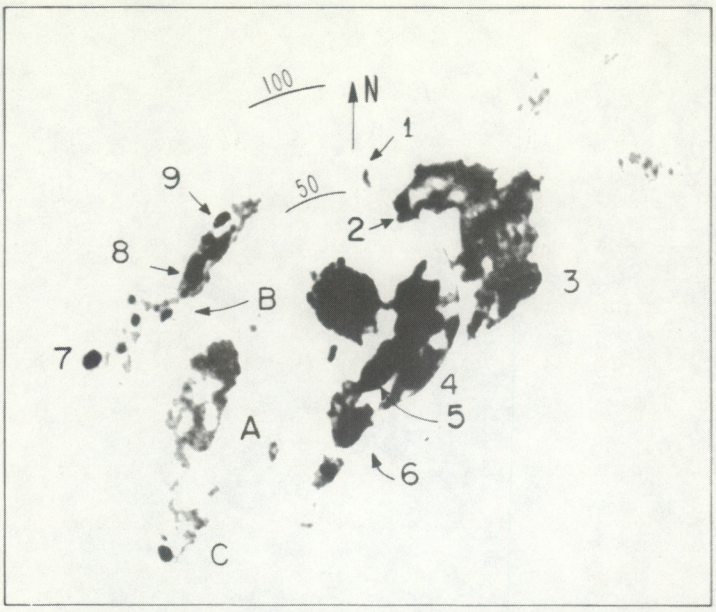

Figure 28. Radar Frame Nº 5596
April 29, 1970 2220 GMT

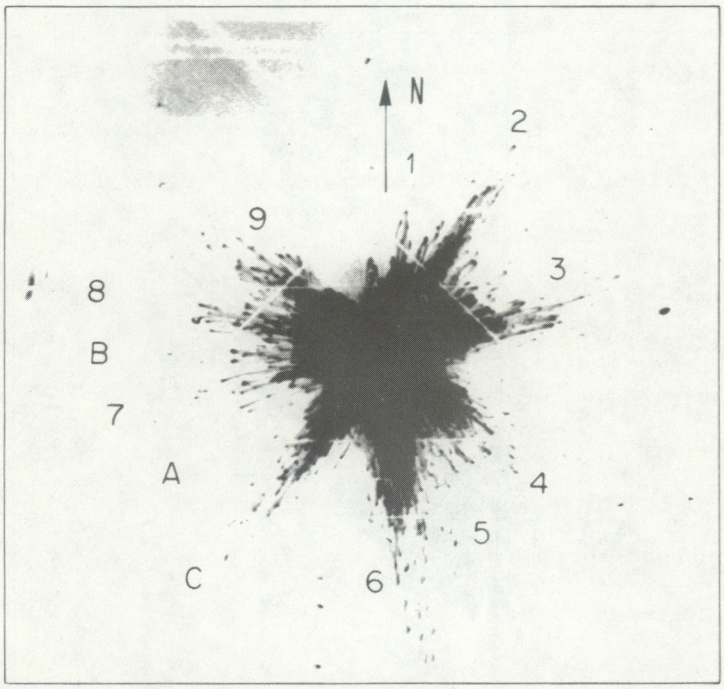

Figure 29. Atmospherics Direction of Arrival
April 29, 1970 2223-2240 GMT

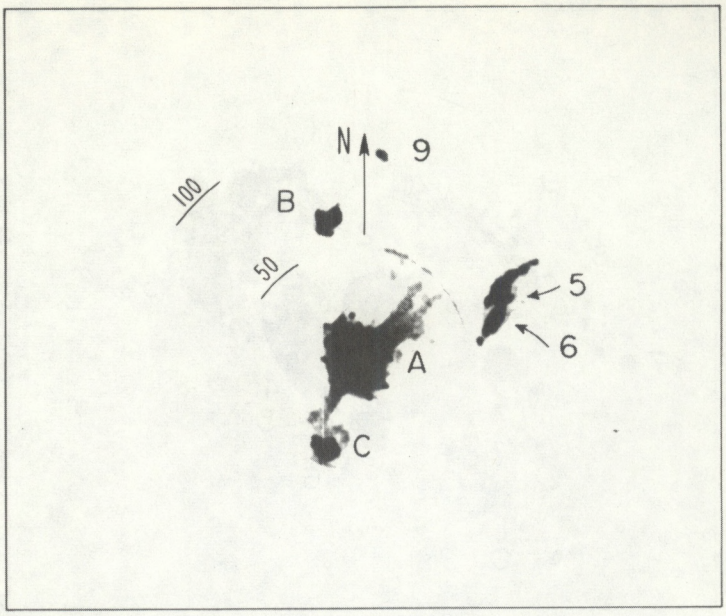

Figure 30. Radar Frame N°. 6090
April 30, 1970 0104 GMT

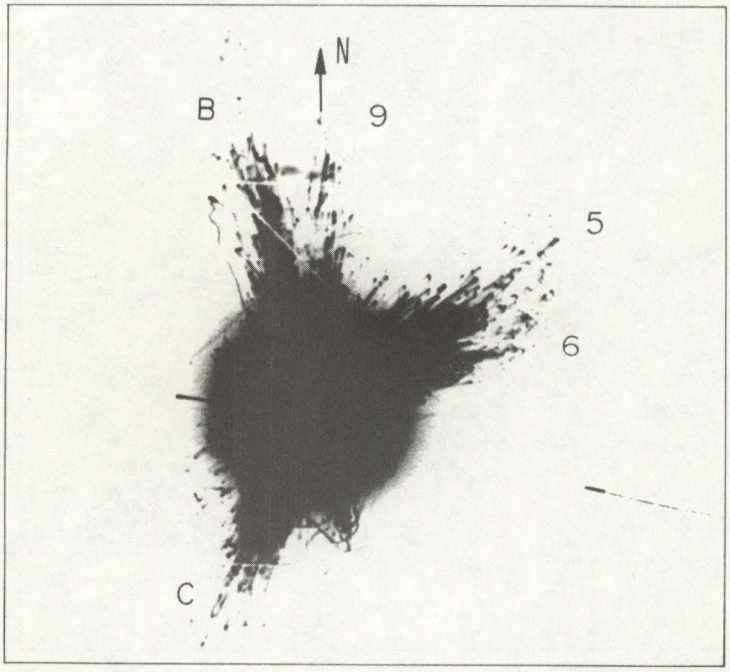

Figure 31. Atmospherics Direction of Arrival
April 30, 1970 0045-0105 GMT

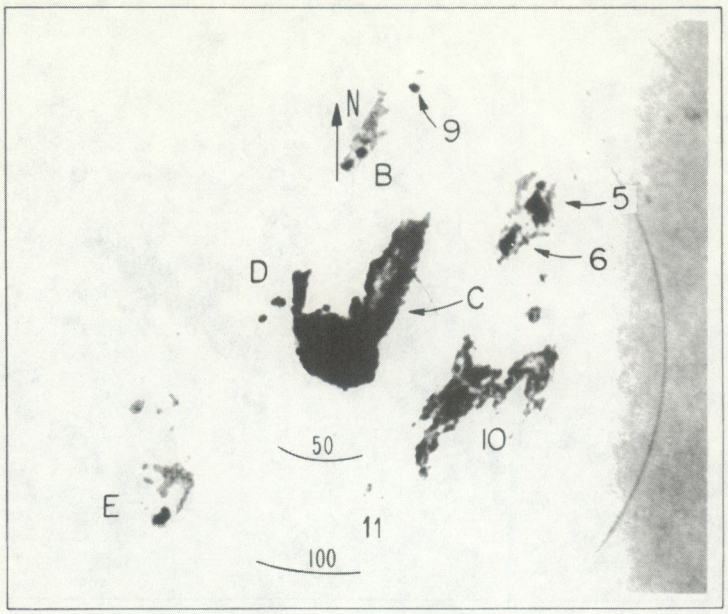

Figure 32. Radar Frame N° 6262
April 30, 1970 0202 GMT

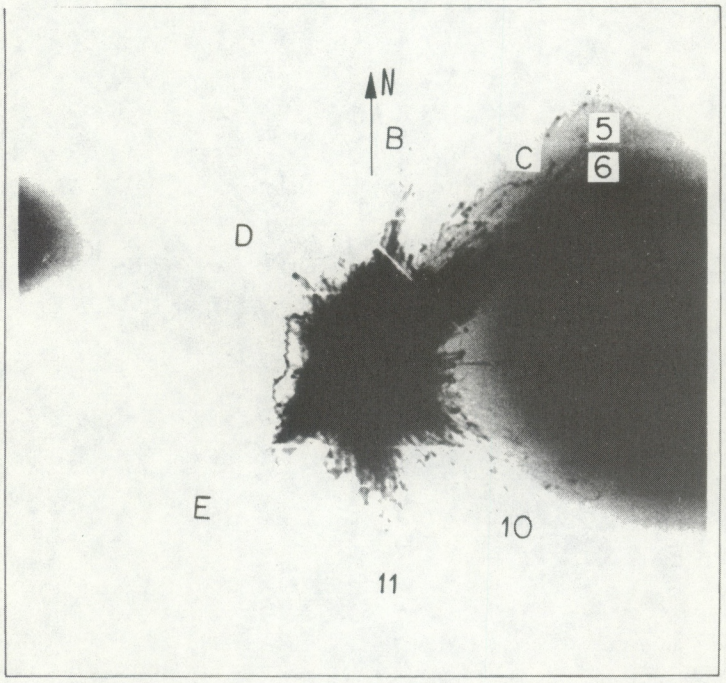

Figure 33. Atmosperics Direction of Arrival
April 30, 1970 0145-0205 GMT

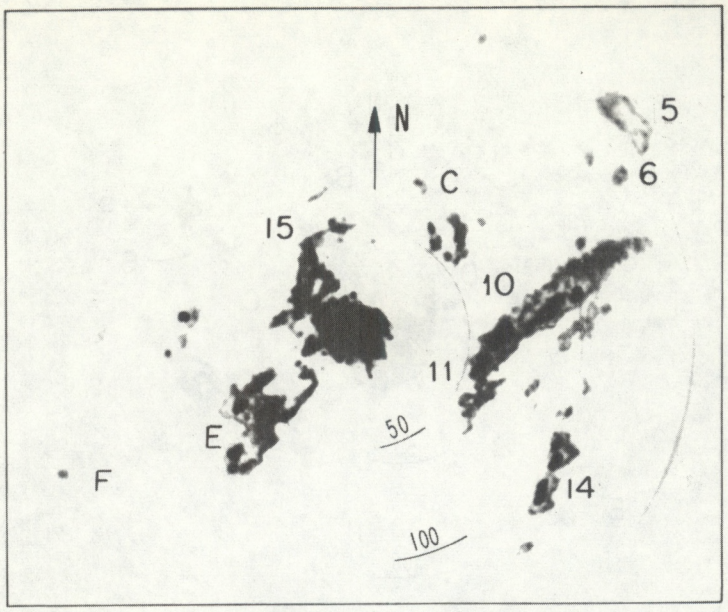

Figure 34. Radar Frame N° 6440
April 30, 1970 0302 GMT

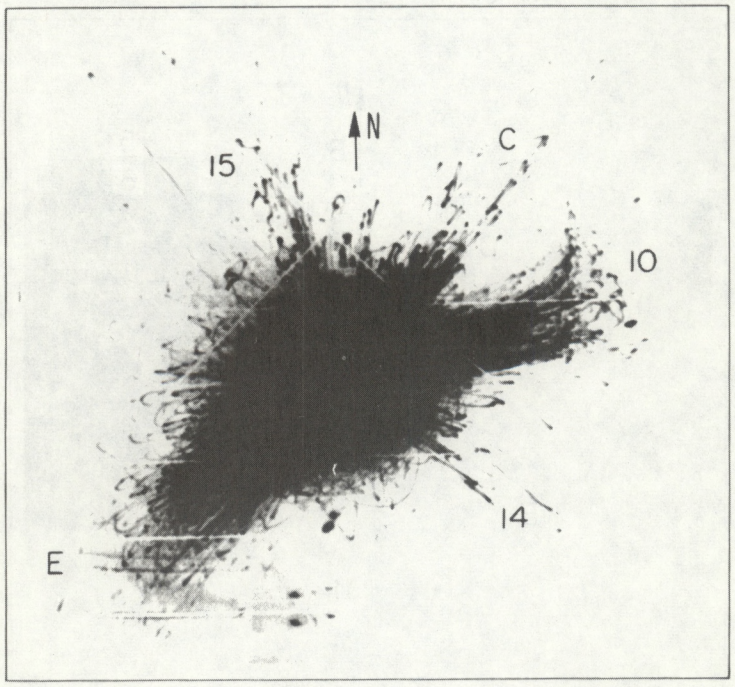

Figure 35. Atmospherics Direction of Arrival
April 30, 1970 0305-0330 GMT

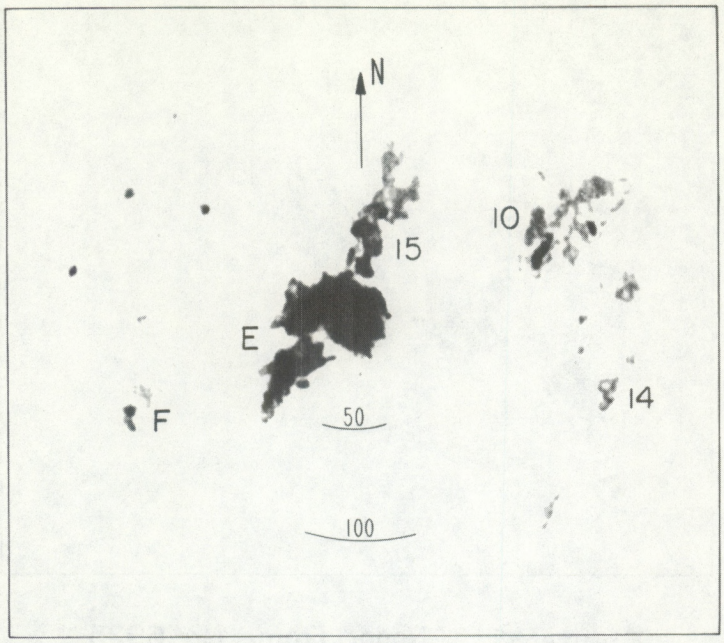

Figure 36. Radar Frame N° 6622
April 30, 1970 0403 GMT

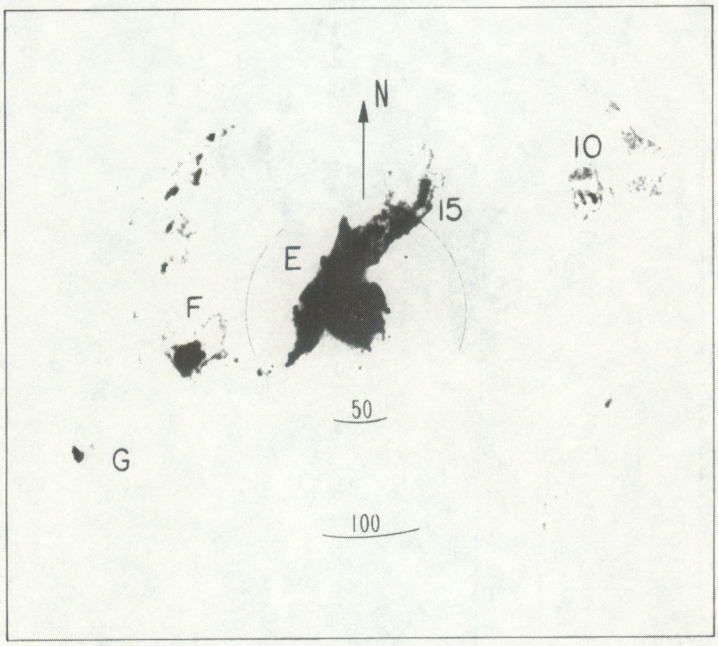

Figure 37. Radar Frame N° 6775
April 30, 1970 0450 GMT

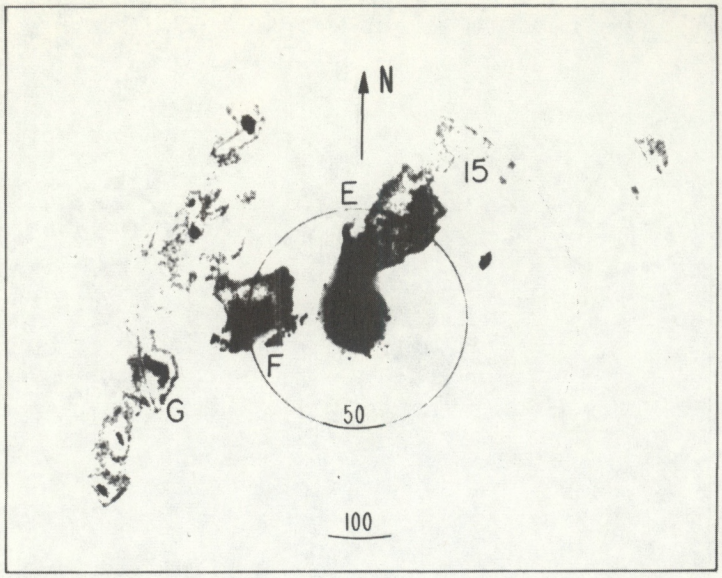

Figure 38. Radar Frame N° 6925
April 30, 1970 0545 GMT

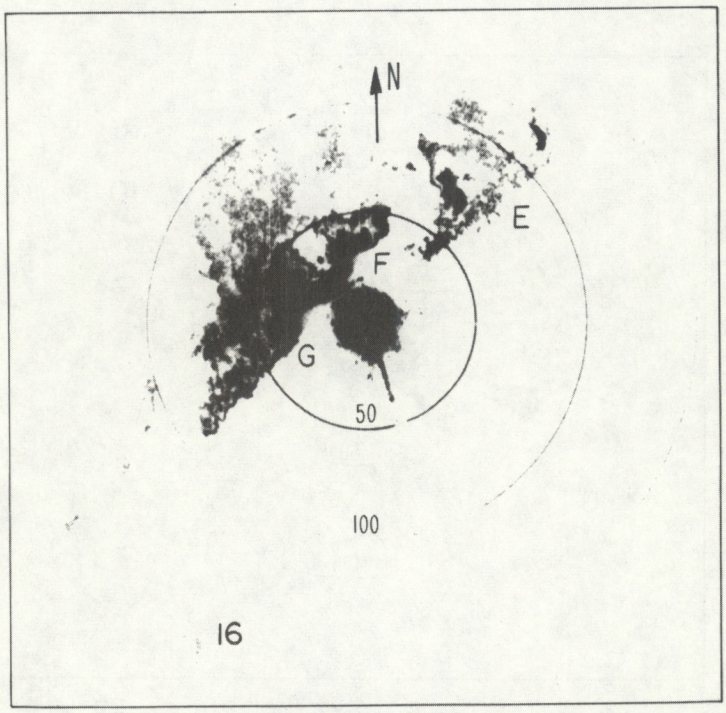

Figure 39. Radar Frame N° 7147
April 30, 1970 0659 GMT

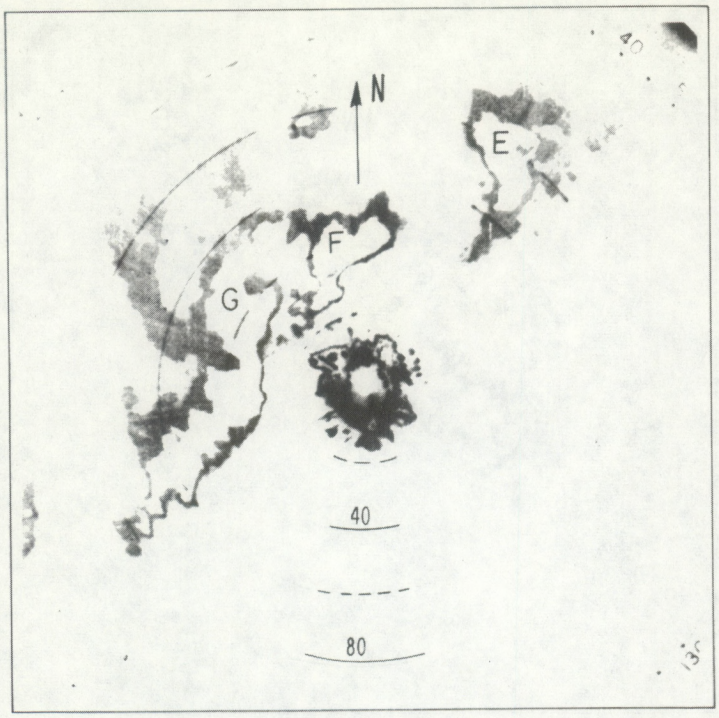

Figure 40. Radar Frame N° 0930
April 30, 1970 0703 GMT

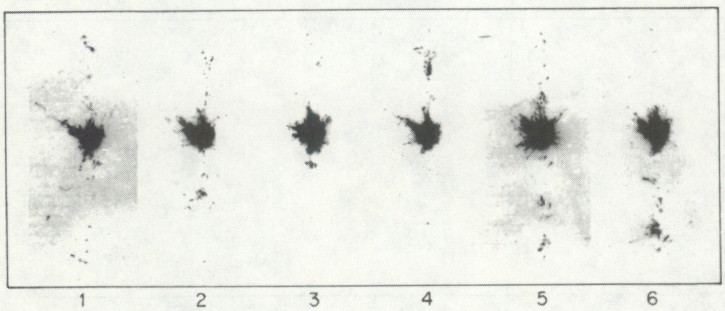

Figure 41. Atmospherics Direction of Arrival
April 30, 1970 0704 GMT

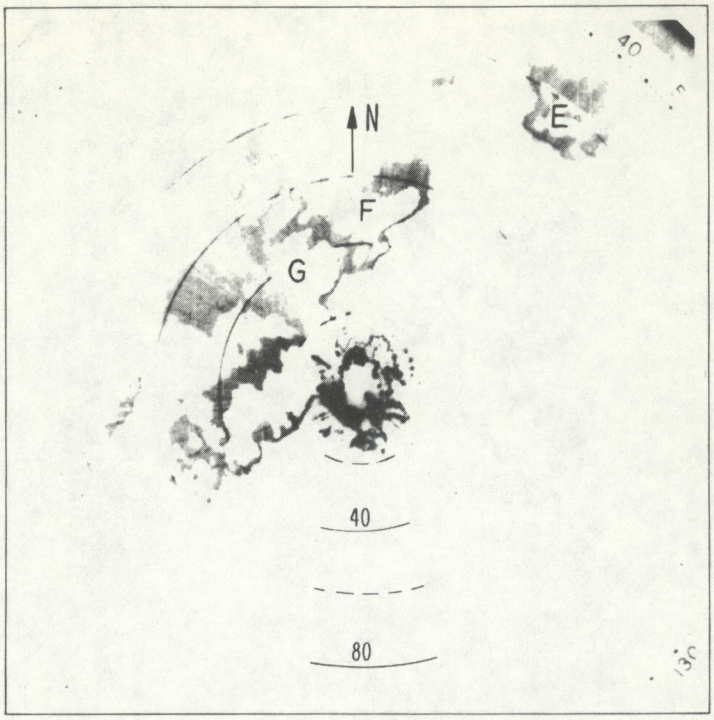

Figure 42. Radar Frame N° 1012
April 30, 1970 0730 GMT

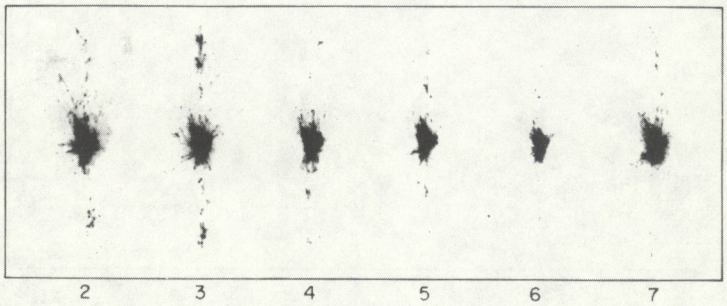

Figure 43. Atmospherics Direction of Arrival
April 30, 1970 0733 GMT

Atmospheric rate data for slow time constant responses during the period 2211-2234 GMT are shown in figure 44. Activity was very slowly increasing during this period with energy arriving from almost all directions as was indicated in figure 29. Channel 31 was occasionally unstable and also affected by some type of noise or interference during this and other periods for this date. There was also some interference noted on channel 32.

Figure 45 rate data for slow time constants show a period of 10 minutes or so around 0000 GMT when a small increase in activity was observed. Although this was an insignificant enhancement of the atmospheric rates, a detail slab of data near 0002 GMT was selected as an example and presented in figure 46.

No significant changes in atmospheric rates occurred until a general increase in activity began around 0350 GMT, as shown in figure 47, for fast time constant data. Some relatively nearby lightning discharges were indicated throughout this period from the potential gradient data on channel 38. These discharges and most of the small background rate activity were most likely produced within the leading portion of storm E as shown in figure 36. Detail rate data shown in figure 48 from around 0355 GMT were selected to show the general appearance of the bursts structure during the increase in activity, with a few large individual discharge rates included.

The fast time constant rate data presented in figure 49 mainly represents the activity associated with storms E and 15 as shown on the radar frame in figure 37. The potential gradient changes around 0500 GMT on channel 38 and corresponding large rate bursts most likely resulted from lightning discharges in the southern part of

storm E. Variations on the magnetic records, channels 39 and 40, at about 0501 GMT were produced by fluctuations on the A.C. power lines.

Two periods for a detail data presentation were selected from data shown in figure 49. The first period, around 0506 GMT, was chosen to represent the peak of the activity most likely associated with storm E. The second period selected 20 minutes later was definitely during the time when activity from storm E was decreasing. There seems to be little differences in the characteristics of the rate data between these two periods except that there are fewer low level rate pulses observed in figure 51 compared to figure 50, especially for the higher frequency channels.

A further selection of data from channels 23 through 29 was made from figure 51 for presentation on an even more expanded time base. A 10-second segment of this data is shown in figure 52. These data channels are from the 1 MHz and 3.16 MHz bands and represent the rate of electromagnetic pulses radiated during a lightning discharge that occurred during the period 28-29 seconds after 0526 GMT. It is of interest to note that the rate of atmospherics that activate channel 26 sustained a level of about 100,000 for half a second or so.

The atmospheric fast time constant rate data observed during the Oklahoma City tornadoes are shown in figure 53. The enhancement in the frequency of the rate bursts is not very spectacular nor are there noticeable changes in rates during this 40-minute period. It should be remembered, however, that one or more tornadoes were reported to have been in existence during this entire period. Atmospheric rates did reach a broad maximum around 0725 GMT and thereafter began a decrease that continued for the next hour. Notice

that no nearby lightning discharges were indicated to have locally occurred from the potential gradient record, channel 38. The tape deck recording channels 11 through 16 was inoperative during this period.

The variations on the magnetic field records shown on channels 39 and 40 between 0725 and 0735 GMT were produced during voltage fluctuations on the A. C. power line. It was later determined that these variations occurred when power was being disrupted in Oklahoma City by the second tornado and causing circuit outages from some of the main substations associated with supplying power on an electrical loop through Norman.

An examination of the detail data taken at 0723 GMT and presented in figure 54 does not reveal a particularly large enhancement in rate data. In fact, the levels of the atmospheric rates shown in figure 50 during the nearby passage of storm E at about 0500 GMT indicate a slightly higher level of activity than is inferred from the figure 54 data.

It was obvious by 0800 GMT that severe activity was over in the central Oklahoma area and that thunderstorms were decreasing in intensity. Expanded time base fast time constant rate data at 0810 GMT, presented in figure 55, shows that individual bursts of atmospherics were becoming more easily recognized at rates elevated above the many small rate bursts. The tendency for the small background burst activity to decrease and the large bursts to become more infrequent, indicative of the decaying state of a thunderstorm, continued until discrete bursts of atmospherics were occurring about once each minute by 0830 GMT.

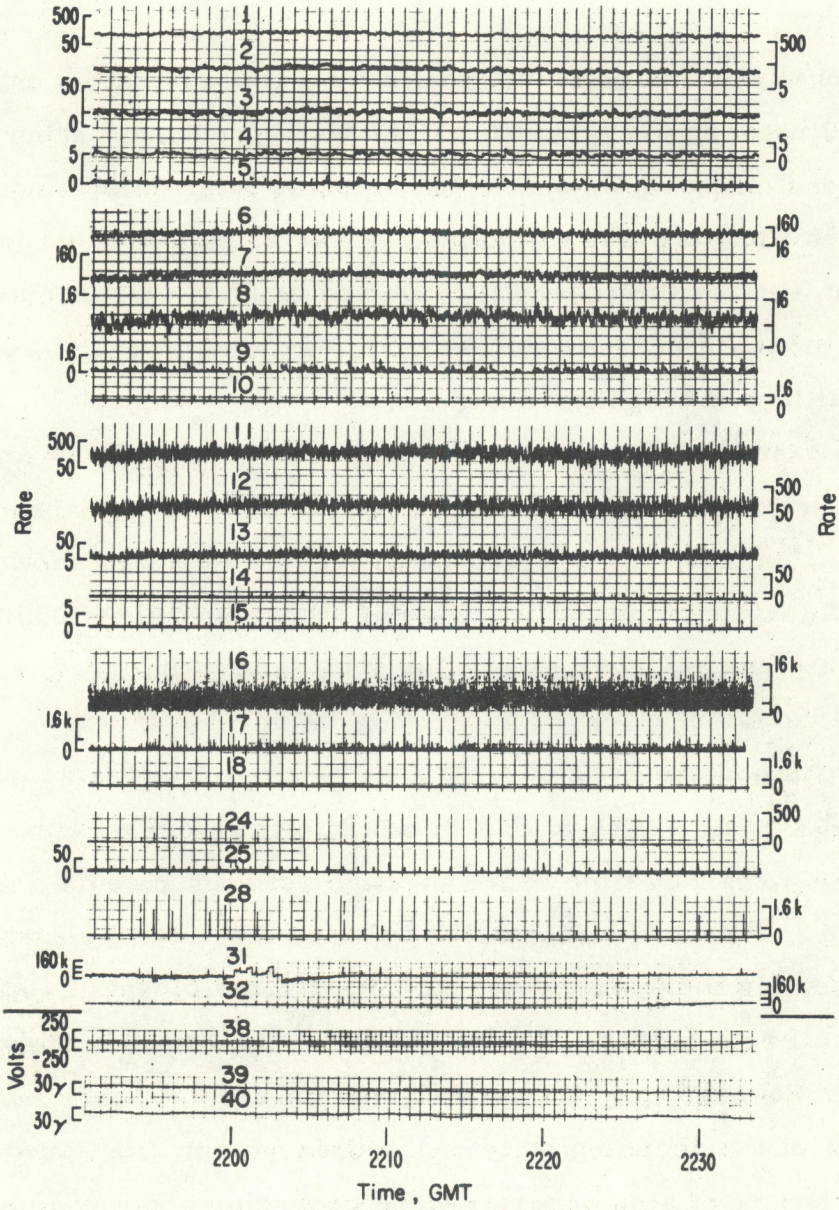

Figure 44. Atmospherics Rate Data

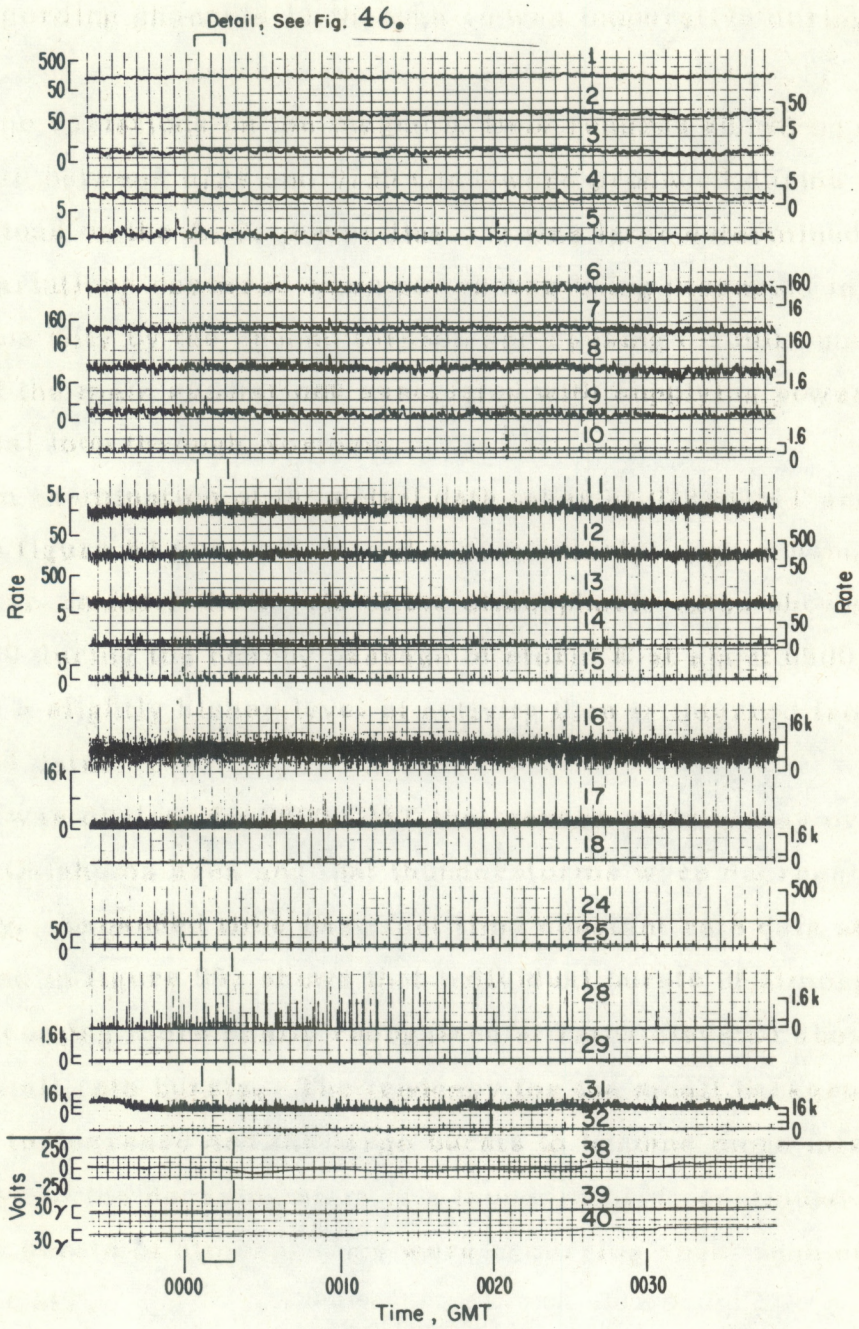

Figure 45. Atmospherics Rate Data

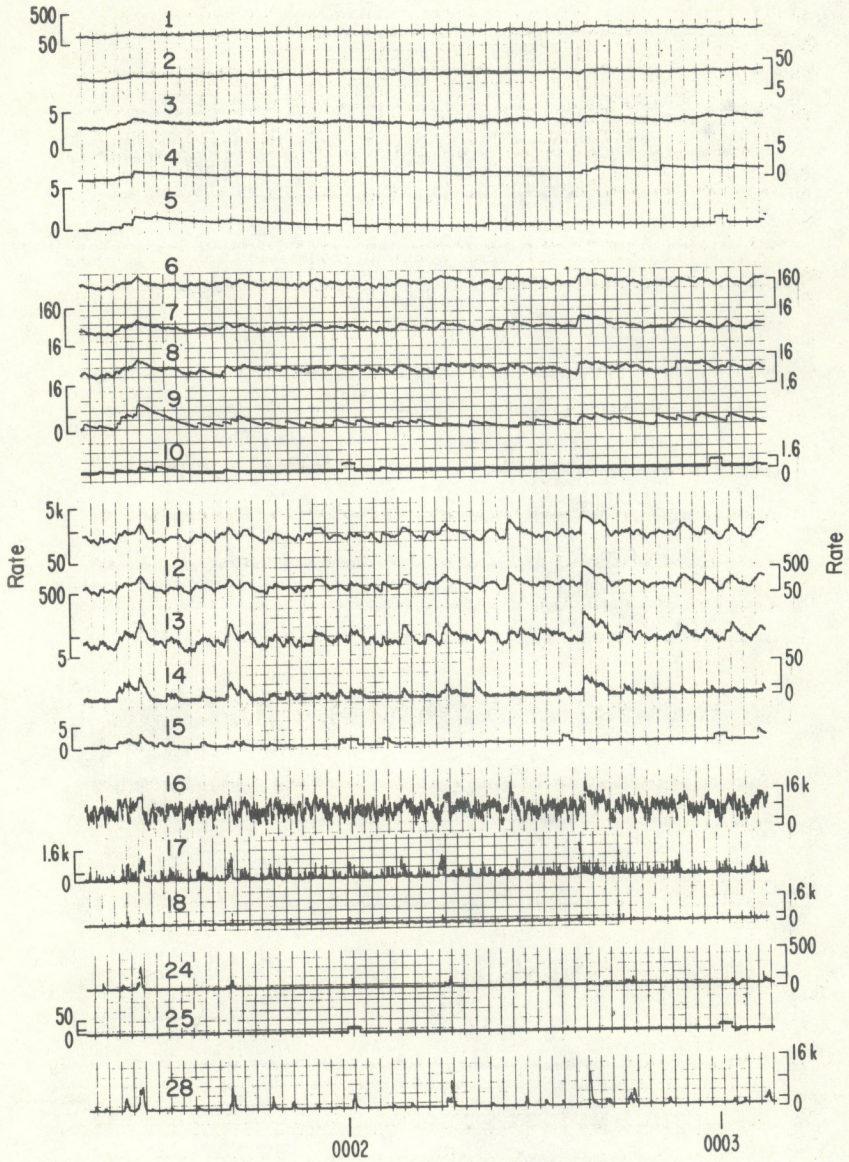

Figure 46. Atmospherics Rate Data, Detail from Fig. 45.

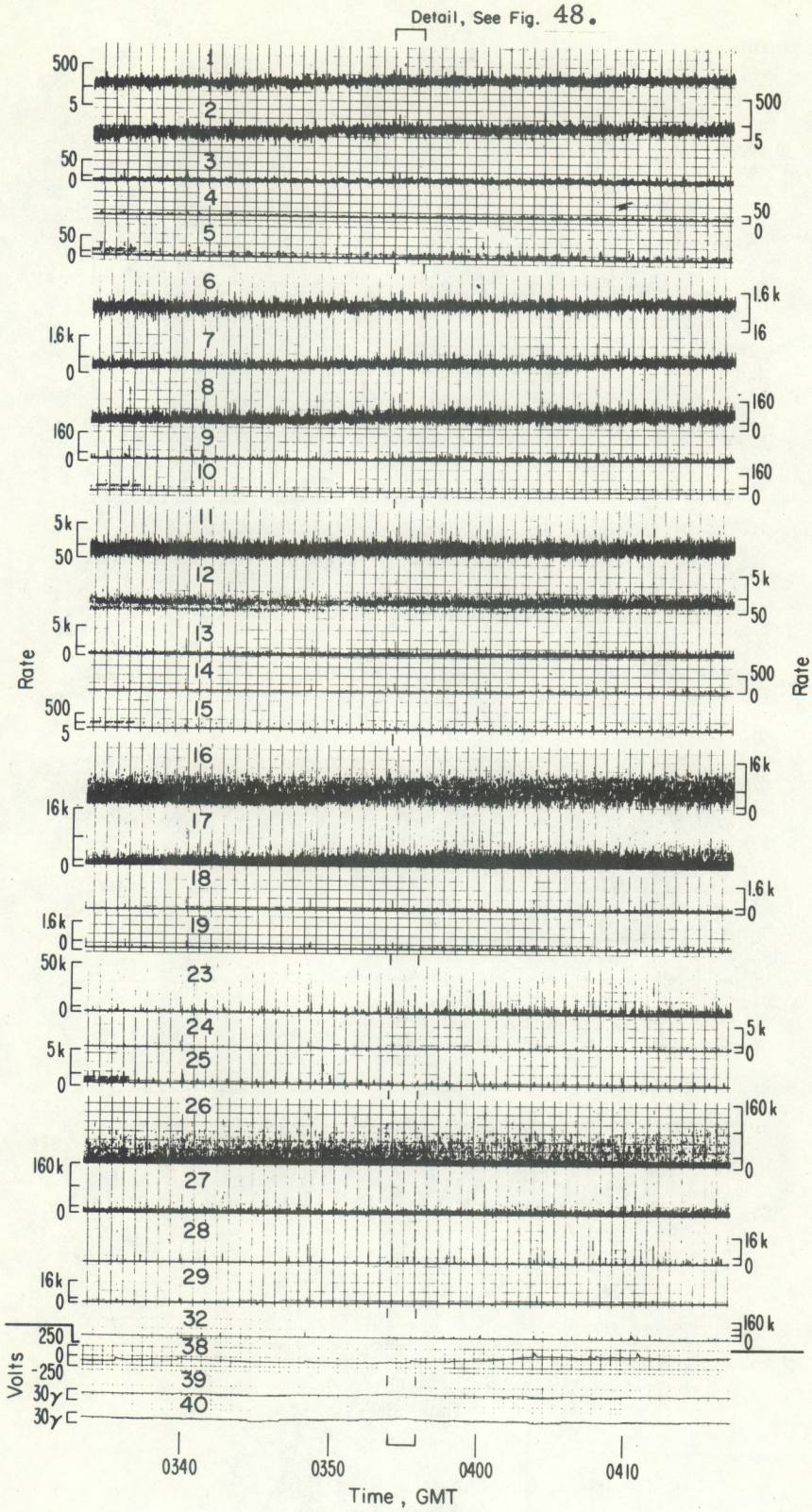

Figure 47. Atmospherics Rate Data

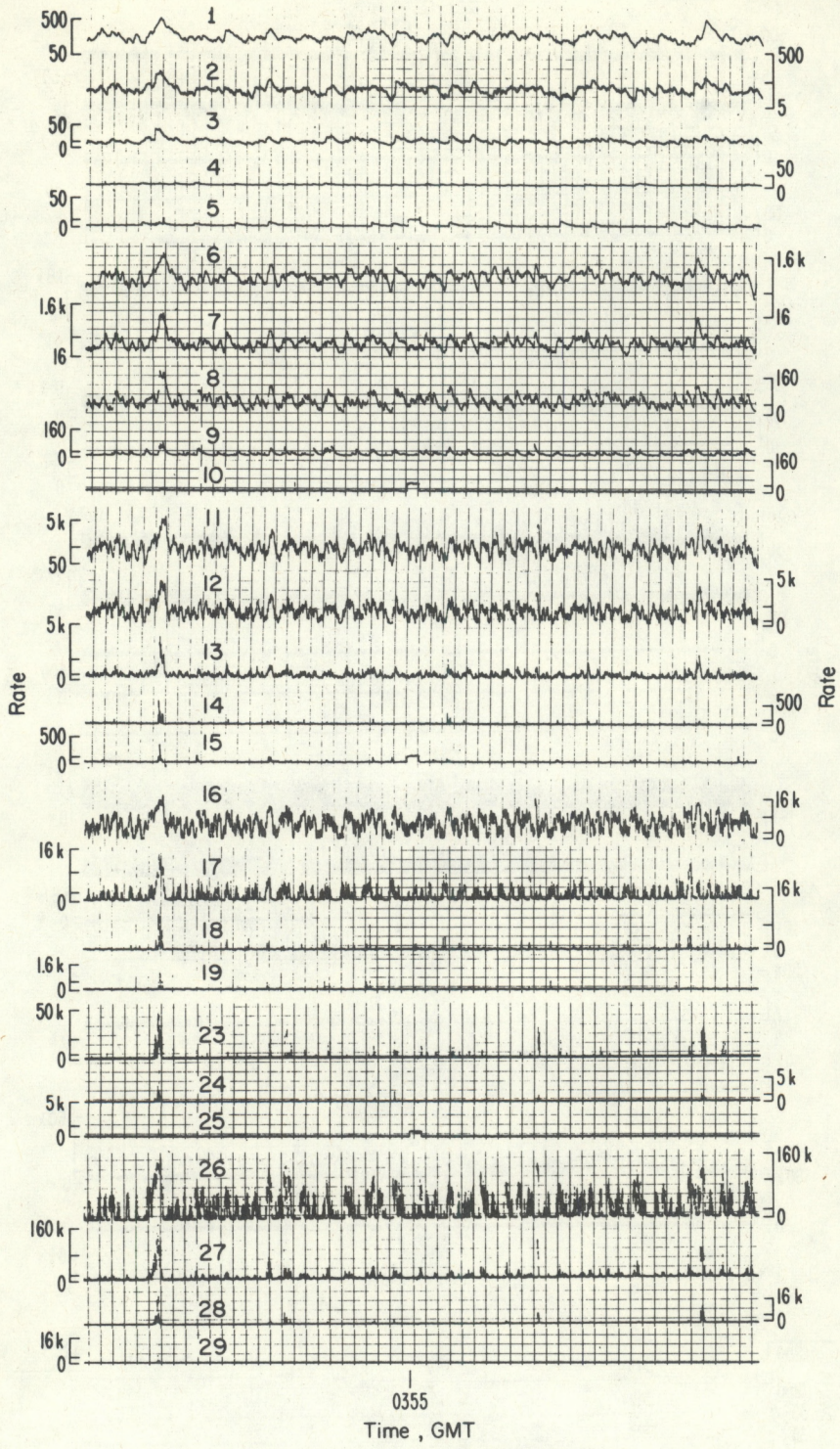

Figure 48. Atmospherics Rate Data, Detail from Fig. 47.

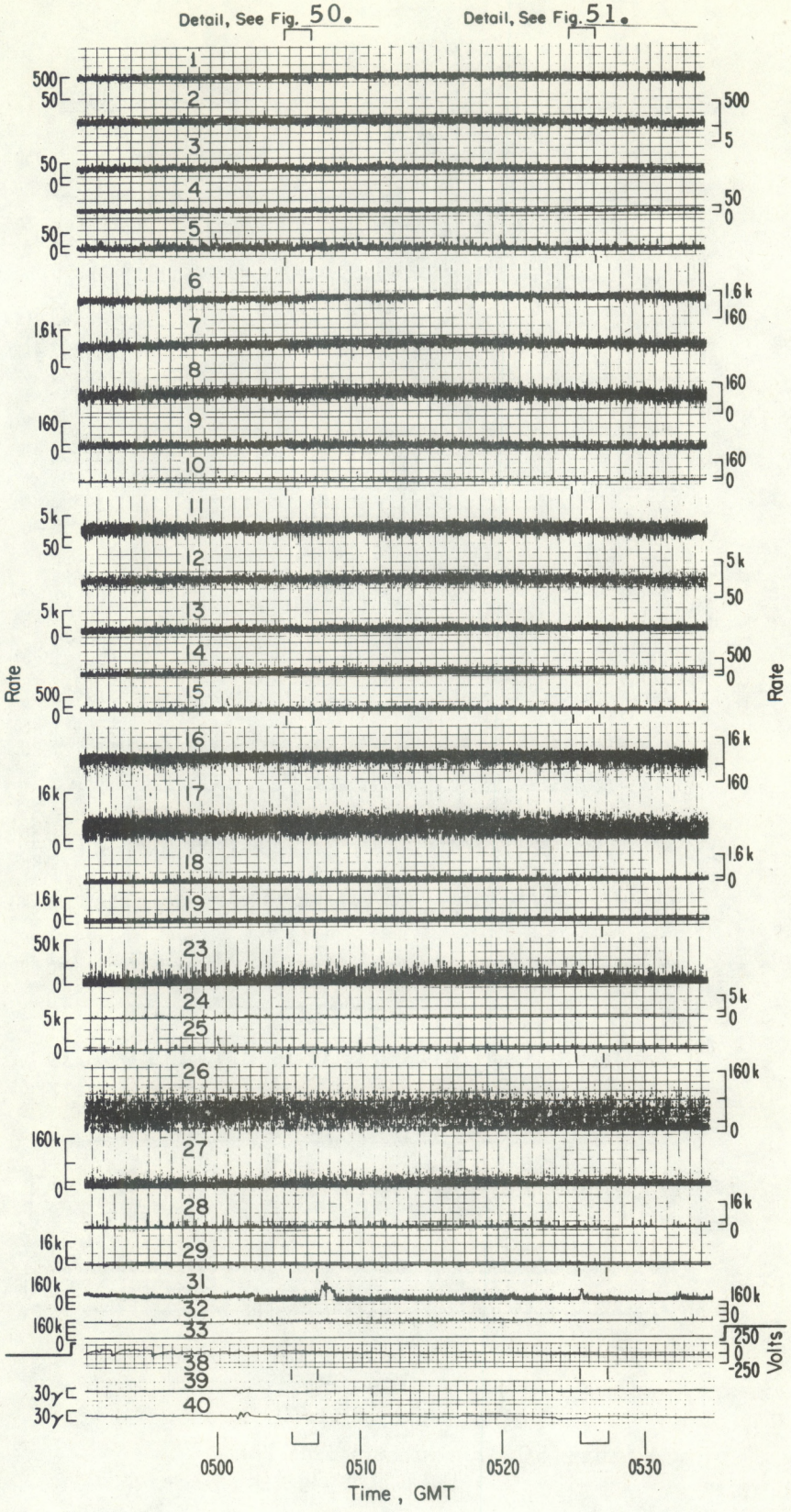

Figure 49. Atmospherics Rate Data

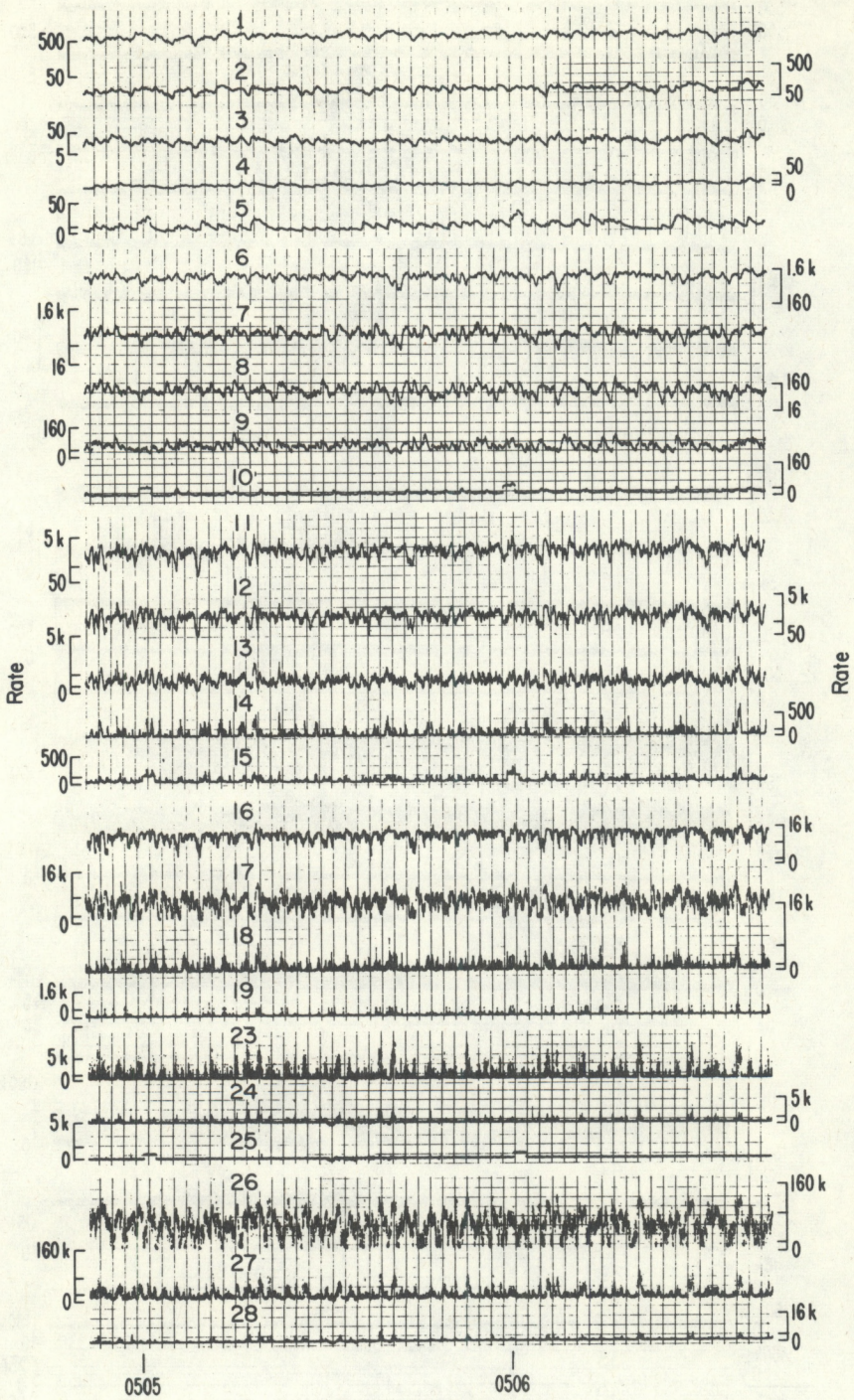

Figure 50. Atmospherics Rate Data, Detail from Fig. 49.

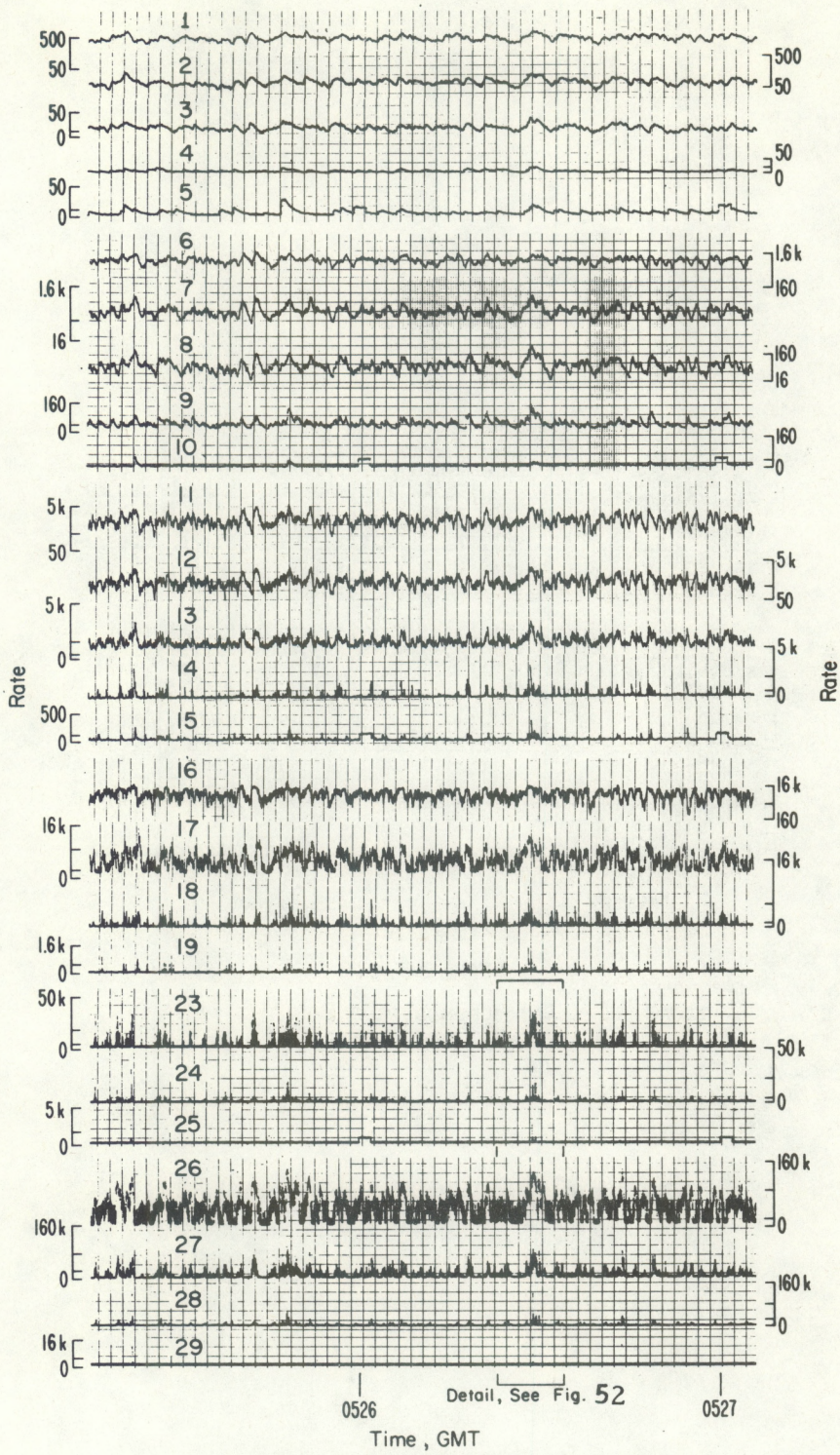

Figure 51. Atmospherics Rate Data, Detail from Fig. 49.

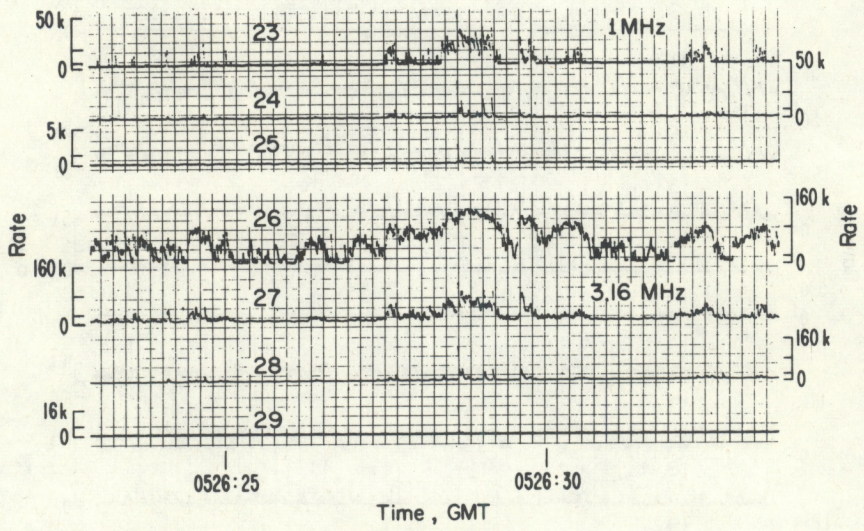

APRIL 30,1970

Figure 52. Atmospherics Rate Data, Detail from Fig. 51.

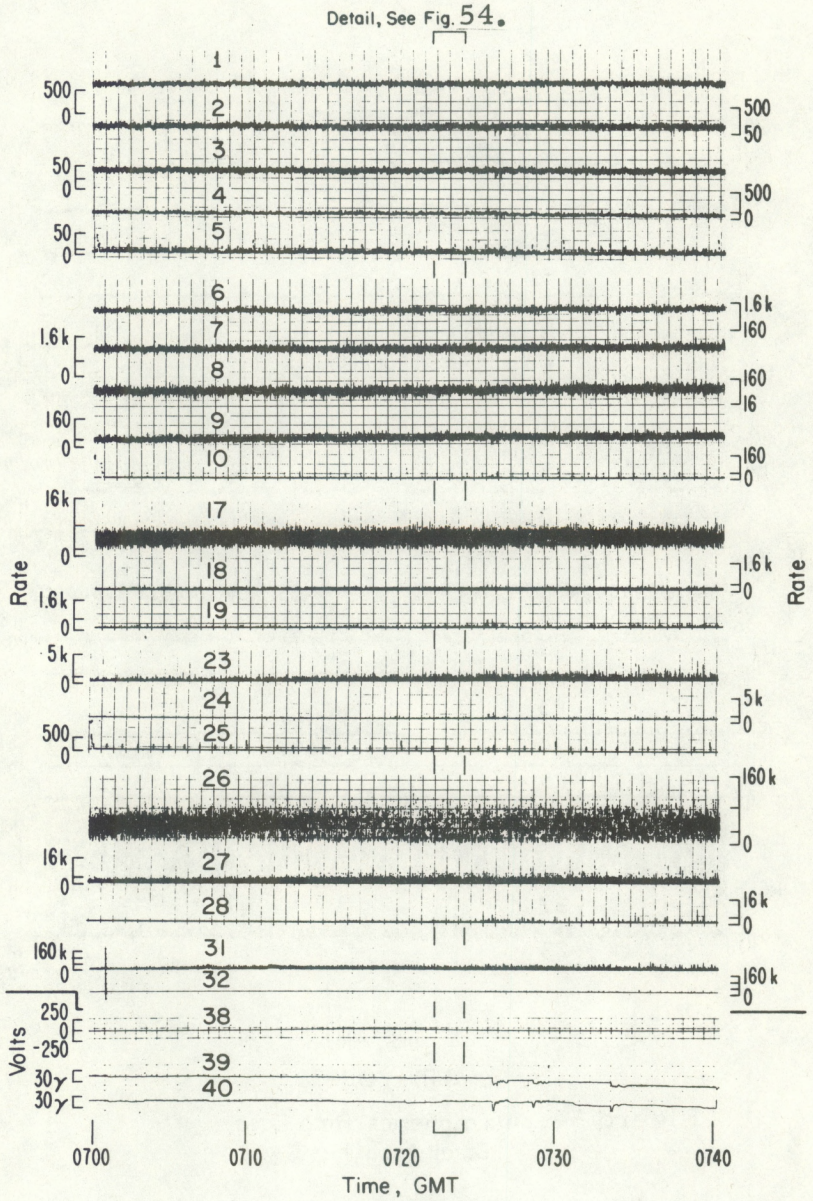

APRIL 30, 1970

Figure 53. Atmospherics Rate Data

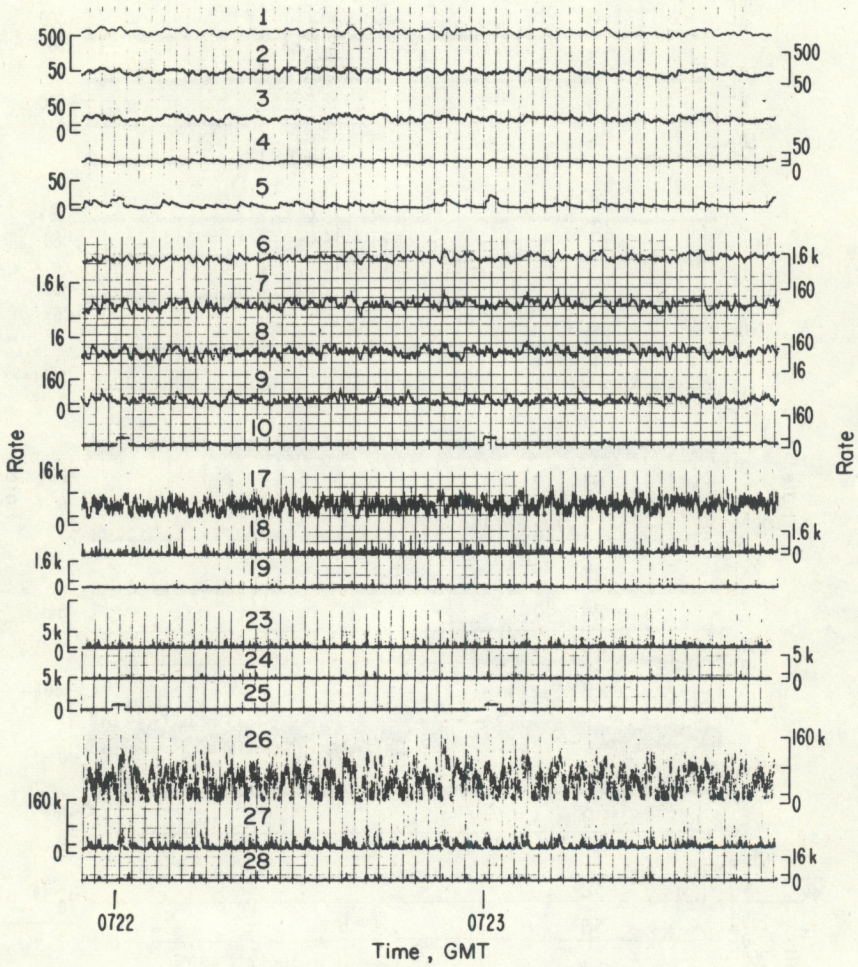

APRIL 30, 1970

Figure 54. Atmospherics Rate Data, Detail from Fig. 53.

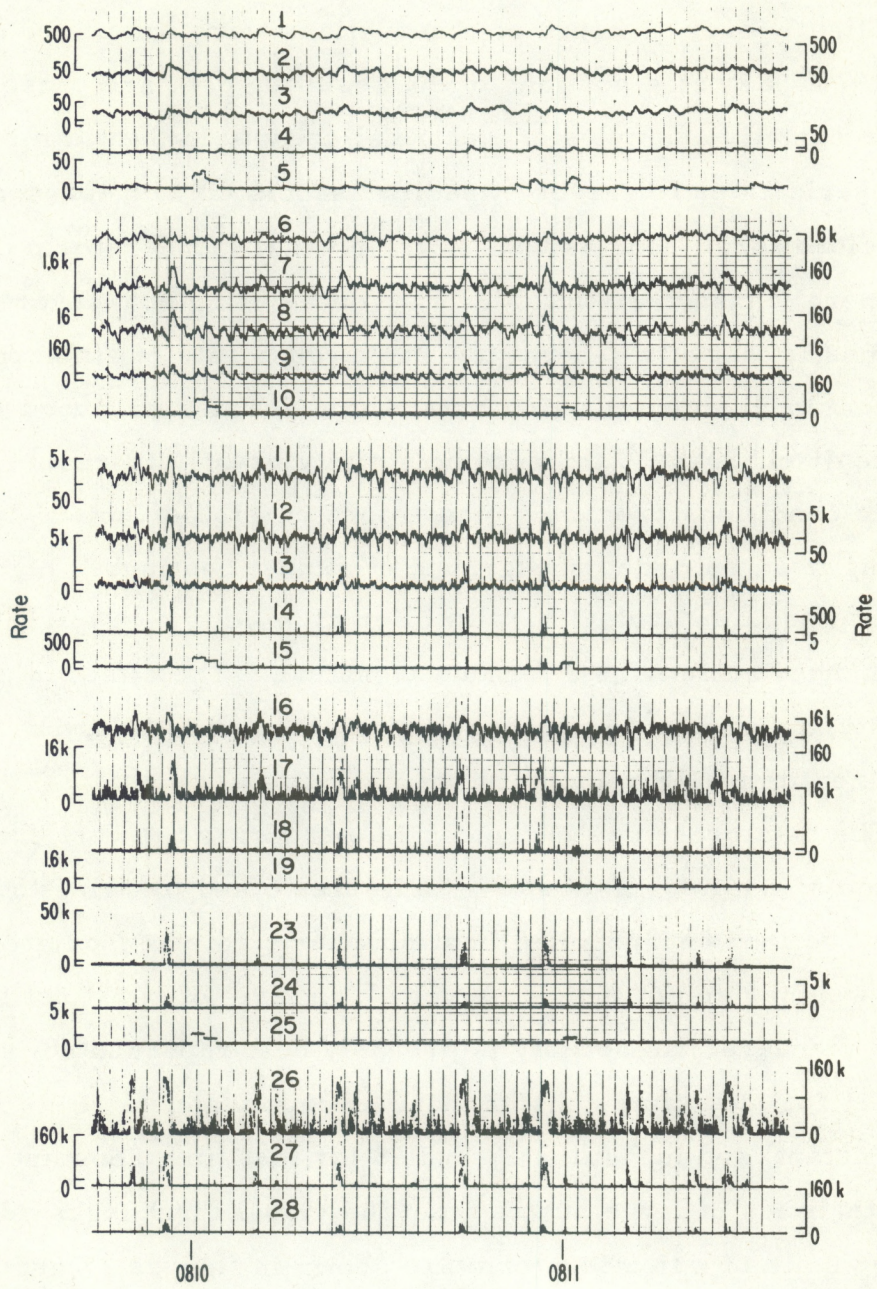

Figure 55. Atmospherics Rate Data, Expanded

4. DISCUSSION

Slightly over 47 hours of observations were completed during April 1970. Selected portions of the resulting data are presented here as representative samples of electrical activity in the form of atmospheric rates for severe weather associated with tornadoes and funnel cloud formations as well as for normal thunderstorm conditions. The general characteristic of the rate data during non-severe conditions is that of a general low background rate of atmospherics with occasional short duration bursts of high rates produced by discrete discharges. Atmospheric activity greatly increases during tornadic conditions producing many more bursts per unit of time and resulting in an enhanced background of almost continuous high rate with little or no individual bursts. For simplicity, we might refer to this enhanced activity as a tornado signature. The effect is not generally apparent at lower frequencies, below 100 kHz, but is easily recognized in the HF region.

The data presented in figures 14 and 15 are the best examples of a tornado signature. Data shown in figures 5 and 6 during the period of a well defined enhancement in atmospheric rates associated with severe weather do not indicate a very high level of burst activity. Normal thunderstorm activity is probably best represented in figures 45 and 46 for slow time constant data (except channels 16-19 are fast time constant) and in figures 47 and 48 for fast time constant data. Characteristics of large bursts from individual discharges during the decaying state of a thunderstorm are shown in figures 27 and 55.

During the month of April when the atmospheric site was operational, there were 3 tornadoes, 2 tornado funnels and 1 reported tornado later downgraded to a severe windstorm for a total of

6 tornadic conditions within 100 km of NSSL. There were also 8 local non-severe thunderstorms observed either within 30 km or with potential gradient changes exceeding 50 volts during the same period. Using the simple subjective criterion for a tornado signature which include the characteristics shown in figures 5 and 14, 5 out of 6 tornadic periods were identified, and one reported tornado was missed. Four thunderstorms were indicated as being severe causing a false alarm, and 4 other thunderstorms produced no atmospheric rate enhancement. A somewhat more rigid criterion would have resulted in one reported tornado being missed but would have produced a false alarm for only one thunderstorm out of the 8.

As indicated in the introduction, no definite conclusions will be attempted at this time. A companion report will be forthcoming to present the atmospheric rate data for the month of May 1970. Further observations will be made during the spring tornado season in 1971 at two locations using modified receiving equipment. A final evaluation of all the data will be made and reported after that time.

The variability in a number of critical parameters for different tornadoes must be measured and the maximum distance to which these parameters are reliable must be determined. The data reported herein during April 1970, definitely indicate that peculiar electrical activity was associated with most tornadoes and funnel cloud formations observed within 100 km. It is hoped that new techniques can be devised from the results of these efforts to aid in the identification and tracking of tornado activity and severe storms, and to reduce the loss of life and property through improved storm warnings.

5. ACKNOWLEDGMENTS

I wish to thank H. Burdick for much of the equipment design and construction and for assisting with the observations, and also thank the many individuals in the NSSL that helped in support of this work during the spring observations. The author was associated with the Institute for Telecommunication Sciences, Environmental Science Services Administration through the period of data collections. The observations for this work could not have been successfully completed without the extra financial support received from NSSL.

6. REFERENCES

Biggs, W. Gale, and Paul J. Waite (1970), Can TV really detect tornadoes?, Weatherwise 23, No. 3, 120-124.

Bradley, P. A. (1965), The VLF energy spectra of first and subsequent return strokes of multiple lightning discharges to ground, J. Atmosph. Terr. Phys. 27, 1045-1053.

Braham, R. R. Jr. (1952), The water and energy budgets of the thunderstorm and their relation to thunderstorm development, J. Meteorol. 9, 227-242.

Dennis, A. S., and E. T. Pierce (1964), The return stroke of the lightning flash to earth as source of VLF atmospherics, J. Res. NBS/USNC-URSI, Radio Sci. 68D, No. 7, 777-794.

Iwata, A., and M. Kanada (1967), On the nature of frequency spectra of atmospheric source signals, Proc. Res. Institute of Atmospherics, Nagoya Univ. 14, 1-6.

Jones, H. L. (1950), The identification and tracking of tornadoes, URSI Comm. 4 Meeting, April 18.

Jones, H. L. (1959), The identification of lightning discharges by sferic characteristics, Recent Advances in Atmospheric Electricity, 543-556 (Pergamon Press).

Jones, H. L. (1965), The tornado pulse generator, Weatherwise 18, No. 2, 78-80.

Mackerras, D. (1968), A comparison of discharge processes in cloud and ground lightning flashes, J. Geophys. Res. 73, No. 4, 1175-1183.

Muller-Hillebrand, D. (1961), The physics of the lightning discharge, Elektrotechnische Zeitschrift ETZ Issue A, 82, No. A8, 232-249.

Ogawa, T., and M. Brook (1964), The mechanism of the lightning discharge, J. Geophys. Res. 69, No. 24, 5141-5150.

Taylor, W. L. (1963), Radiation field characteristics of lightning discharges in the band 1 kc/s to 100 kc/s, J. Res. NBS, Radio Propagation 67D, No. 5, 539-550.

Uman, M. A., and D. K. McLain (1969), Magnetic field of lightning return stroke, J. Geophys. Res. 74, No. 28, 6899-6910.

Vonnegut, B. (1960), Electrical theory of tornadoes, J. Geophys. Res. 65, No. 1, 203-212.

Waite, P. J., and N. Weller (1969), The Weller method: Tornado detection by television, Proc. of Sixth Conf. on Severe Local Storms, Chicago, 169-171.